ITER Plasma Diagnostics

8th EIROforum School on Instrumentation

C. Ingesson, U. Walach, M. Perez Lasala, C. Sanchez Macua

Overview

- **Diagnostics:**
  - Magnetics (55.Ax) – **Delivered**
  - Magnetics I&C and scientific software (55.A0) – **Delivered**
  - Radial neutron camera (55.B1) – Preparing for **manufacture**
  - Core-plasma Thomson scattering (55.C1) – Completing **design**
  - Collective Thomson scattering (front end) (55.C7) – Preparing for **manufacture**
  - Bolometers (55.D1) – Completing **design**
  - Core-plasma QQCXRS (55.E1) – Completing **design**
  - Equatorial Vis./IR wide-angle viewing system (55.G1) – Preparing for **manufacture** (EQ12) / **design**
  - Diagnostic pressure gauges (55.G3) – Closing FDR, preparing for **manufacture**
- **Other components and common activities:**
  - Cable looms, electrical feedthroughs, divertor RH connector (55.NE) – **Delivered**/**manufacture**/**design**
  - Port integration – Preparing for **manufacture**

In-vessel Cabling

- **Scope of supply**
  - **1250 UHV-terminated mineral-insulated cables**
  - Total length: **7.7 km**
  - **Seven different types** (single core, twisted pair, quad, alumina or silica, thermocouple, diameter, …)
- **Delivery**
  - First delivery in July 2022. Problem with Cu coating and cleaning processes found at SAT – corrected coating process since Apr-2023.
  - Delivery of batches from Jun-2023 until December-2024

Vacuum Vessel Feedthroughs

- **Scope of supply**
  - **75 electrical feedthroughs** for in-vessel cables in VV and divertor
  - Configurations with **1–3 bulkheads**, with **ten variants** of bulkhead (→)
  - Total number of **pins**: 9884
  - Include 3049 lengths of **MI cables** (11.4 km)
  - Prototypes shown at earlier meetings
  - Cable-insertion tool designed and demonstrated (↘) to allow installation at port extension
- **Delivery**
  - 1st batch by Feb-2027
  - 5th batch by Oct-2028

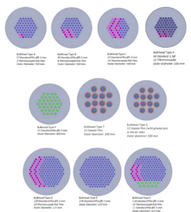

Systems starting manufacture

FDR on whole scope or subsystem closed or almost closed, and manufacturing contract being prepared for launch:

- **Port Integration** (EP01, EP10, UP01, UP03, UP10, UP17) – FDRs closed in Dec-2022, post-FDR modifications being addressed. Preparation for manufacturing on-going.
- **Collective Thomson Scattering (Front End)** – FDR closed Dec-2022. Preparing for manufacturing.
- **Diagnostic pressure gauges** – FDR completed Mar-2024, including I&C – working on chits (e.g. some interface updates, addressing clearances, welding restrictions, radiative heat loads, and fatigue test on Ir foil).
- **Equatorial Visible/IR Wide-Angle Viewing System**

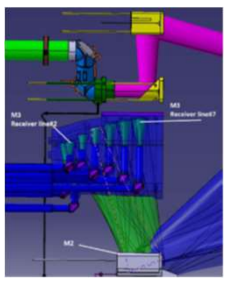

CTS injection and collection layout

CTS split-biased waveguide prototype

Radial Neutron Camera

- **FDR** for **in-port** components **closed. Manufacture in preparation.**
- **PDR** for **ex-vessel** held (Jun-2023) – IS & CM/CMAF in progress (→)
- **Preparing for MRR for fission chambers – delivery** Q4 2024
- **Prototyping and testing of detector technology** (↙ ↘)

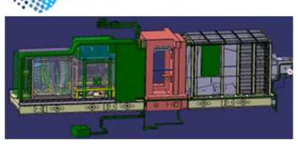

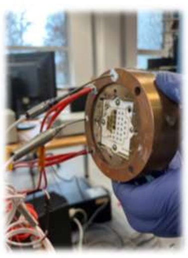

Cividec CVD single-crystal diamond matrix neutron detector has additionally been cycled successfully to 240°C (baking temperature) at IFJPAN.

Prototyping & Testing of preamplifier for CVD diamond detectors successful

Prototyping & Testing He-4 detector on-going (80–100 bar container + PMT)

Magnetic coils

PAs on external Rogowskis, outer-vessel coils and inner-vessel coils had already been completed.

The last remaining:

- Mid-2023: 19 **divertor coils (55.AL)** (+1 spare) delivered after calibration (↙).
- 7 **Diamagnetic compensation coils (55.AG)** according to new design and PCR
  - **Lengthy process**: two types of prescribed braze inadequate (e.g. noticed after MRR that magnetic, or microcracks in sheath of cables in contact with the braze after manufacture). **New Cu-P brazing validated by IO.**
  - Joint F4E–IO manufacturing process agreed: manufacturing of supports, cables and thermocouples (F4E – **completed**), brazing (IO), joining terminations (F4E) and calibration (F4E)

Spin-off: technology (IP) developed on LTCC magnetics sensors applied elsewhere by supplier VIA Electronic

Tangential divertor coil

Toroidal divertor coil

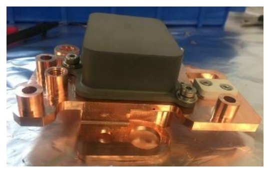

In-vessel Supports

- **Scope of supply**
  - 56000 **clips** of one variant → secure cable tail to VV
  - 9045 **clamps** of 8 variants → hold looms of cables together
  - 500 **junction boxes** of 8 variants → connect different lengths of cables, such as sensor cable looms
- **Delivery** (after implementation of IO PCR)
  - 1st batch by July-2024
  - 2nd batch by Dec-2024

Drawing of a clip

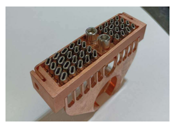

Two types of clamp

Two variants of junction box

In-Divertor Electrical Services

- Contract for **final design and manufacture**
  - Design ongoing, preparing for FDRs (inboard and outboard)
  - Testing platform for inboard design under assembly
  - New approach for **divertor RH connector** (↘)
- **Scope of supply**
  - **Divertor RH connectors**: 13 outboard and 3 inboard
  - 9 –131 cables per divertor cassette } 2300 **cables** in total
  - In-port cable tails
  - **Clips** and **clamps**, and some **junction boxes**

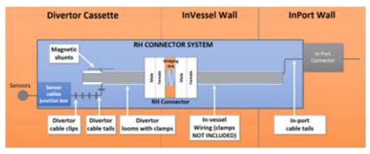

Divertor RH connector under triangular support in disconnected (left) and connected (right) positions

Core Plasma Thomson Scattering

- PDR was held, closure ongoing
- **The preparations included targeted prototyping** of specific sub-components, such as:
  - Optics alignment system (→)
  - Shutter proof-of-principle (↙)
  - Mirror cleaning
  - PIC qualification completed: **shutter valve, secondary window, secondary window valve** (↘)

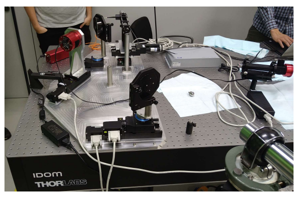

Bolometers

- **Cable-installation templates (CITs) have been delivered to ITER** (↓)
- Preparing for **FDR on port-mounted cameras and sensors** (↙)
- **PDR on VV- and divertor mounted cameras** on-going
  Preparing for **PDR on I&C**. Prototypes of bespoke electronics ongoing (↗)

Prototype voltage source (bottom) —not final form factor and many testing features—connected to digital part of magnetics integrator (top) for ADC.

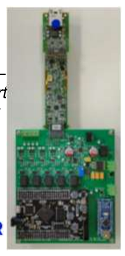

Main part of CITs before packaging (in insert: CAD of assembly)

Design progress of port-mounted bolometer cameras and sensor prototyping was presented recently – **high loads** are still a challenge.
Testing of prototype bolometer sensors agreed at PDR:

- Temperature-dependent calibration ✓
- Steam test ✓
- Thermal-cycling test ✓
- Pressure-wave test ✓
- Pressure-dependent calibration ✓
- **DMS light-flash test** ✓
- **Vibration test** ✓
- **Irradiation test** → in preparation (→)

Left: 5-m long irradiation rig during FAT (encircled: prototype sensors embedded at the far end). On right: DAQ system and 14-m long hoses with cables.

The GIRAFFE Experiment – In Situ Material Tests under Fusion-Relevant Conditions

Hydrogen retention
↓
Embrittlement

THERMO-MECHANICAL LOADS

High heat flux
Mechanical stress

Displacement damage
↓
Embrittlement

PLASMA INTERACTION

Erosion by plasma
Hydrogen retention

NEUTRON IRRADIATION

Displacement damage
Transmutation

Displacement damage
↑↓
Hydrogen retention

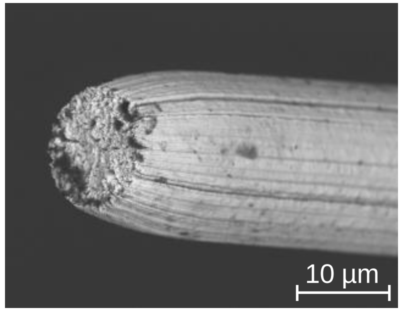

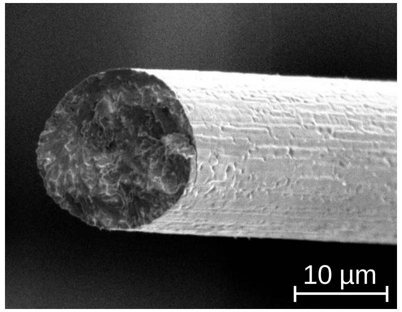

Influence of impurities on the mechanical properties of plasma-facing materials

General-Purpose Irradiated Fiber and Foil Experiment

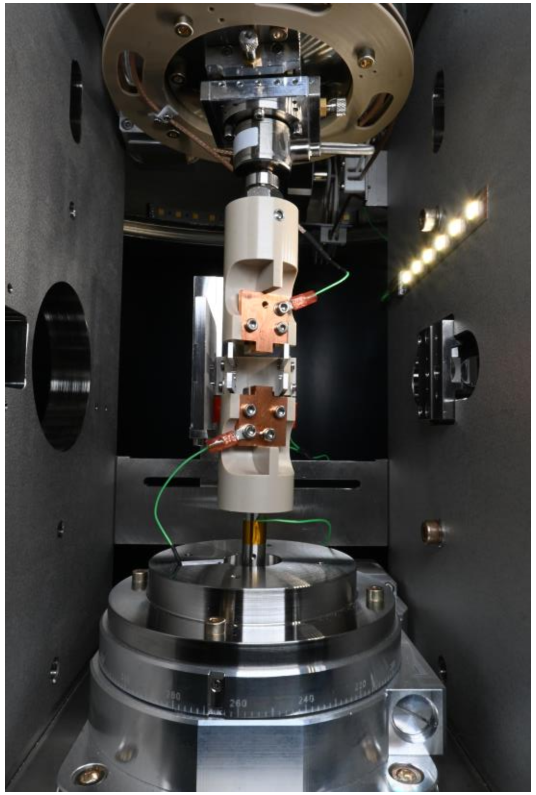

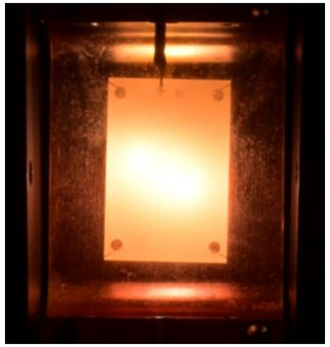

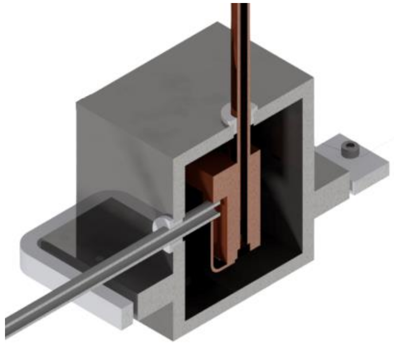

High-precision tensile testing machine at a particle accelerator to simulate the fusion environment

Entering the World of Detector Characterization

esa

Katrin Geigenberger

Master of Physics
(Nuclear-, Particle-, and Astrophysics)

- Focus: Astroparticle Detection
- Worked with
  - Cryogenic Detectors
  - Silicon Drift Detectors
  - Silicon-Photomultiplier

OHB

Internship in Optical AIT

Graduated Aug. 2023

esa Young Graduate Trainee

- Started 01. Sept 2023 @ ESTEC
- Science – Future Mission – Payload Validation
- Characterization of NIR CMOS Detector 'ALFA-N'
- Maintaining Health of the Detector
- Readout Electronics, Data Acquisition, Processing

Latest Work: Near-Infrared CMOS

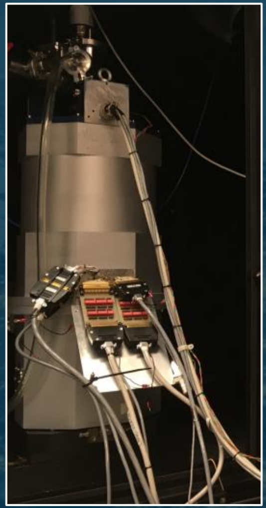

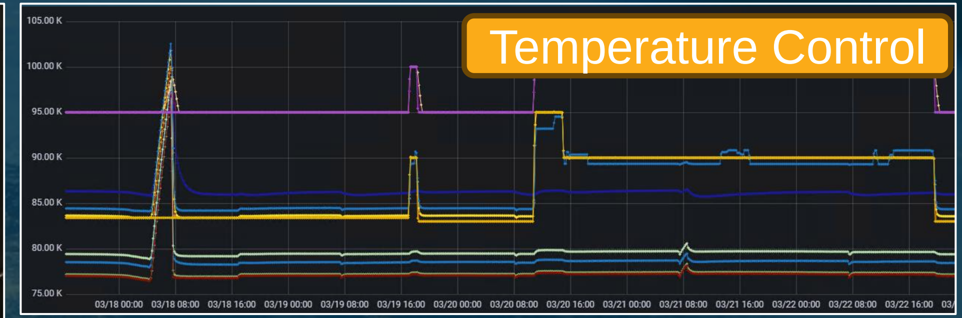

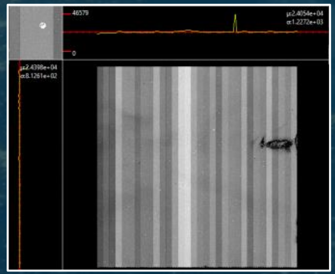

DAQ

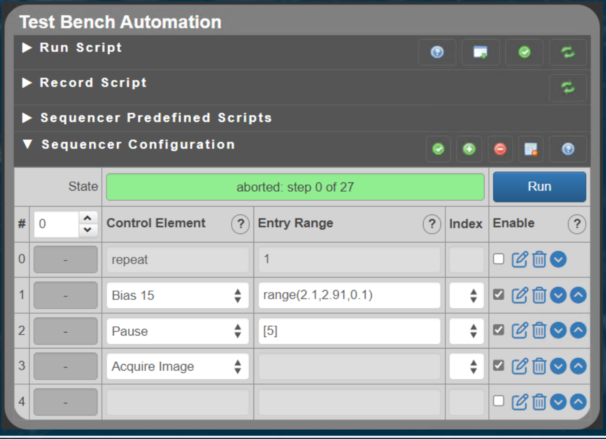

Data Processing

Python

Large Datasets ~50 GB

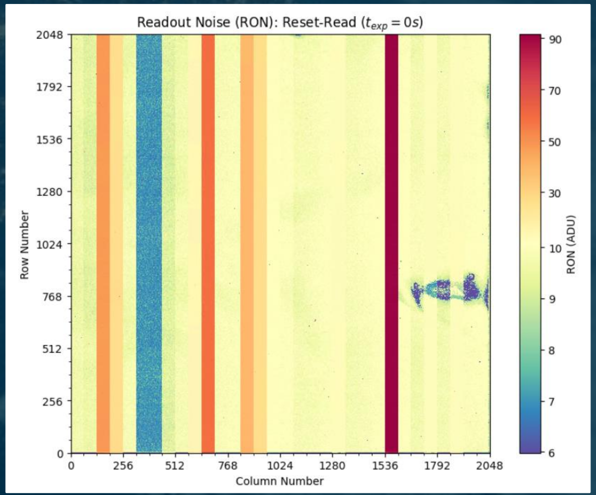

The ScopeSim Ecosystem

Fabian Haberhauer

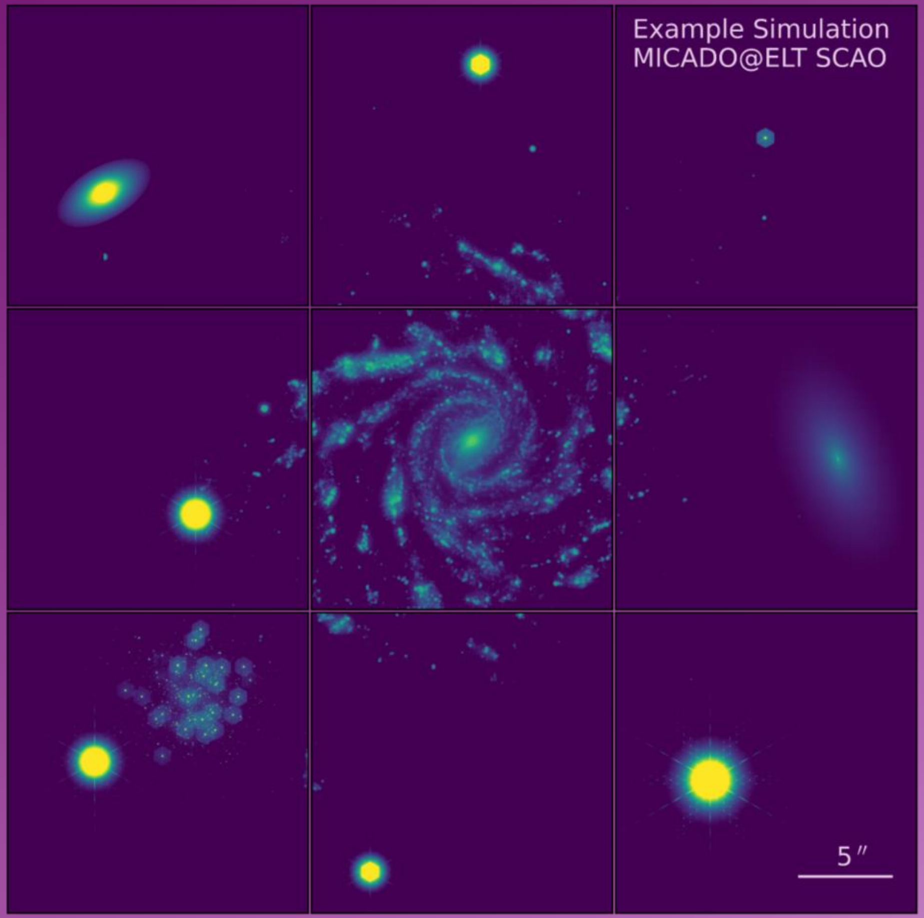

In a nutshell…

- General purpose flexible astronomical observation simulator engine in Python.
- Sequence of phenomenological “effects”.
- Supports imaging, spectroscopy and MOS.
- Description of source object and instrument setup in separate packages (IRDB).
- Auxiliary packages for atmospheric properties and spectra manipulation.

MICADO Main Selector Mechanism MAIT Phase

Jonathan Lange

- **Manufacturing and Procurement:**
  - Developing technical drawings and Bills of Materials (BOMs).
  - Communicating with suppliers and placing orders for the necessary components and materials.
- **Assembly and Integration:**
  - Planning the assembly process, including the coordination of alignment procedures using a Coordinate Measurement Machine (CMM).
- **Testing:**
  - Designing and executing test protocols, such as those involving Giant Magneto-resistance (GMR) sensors.

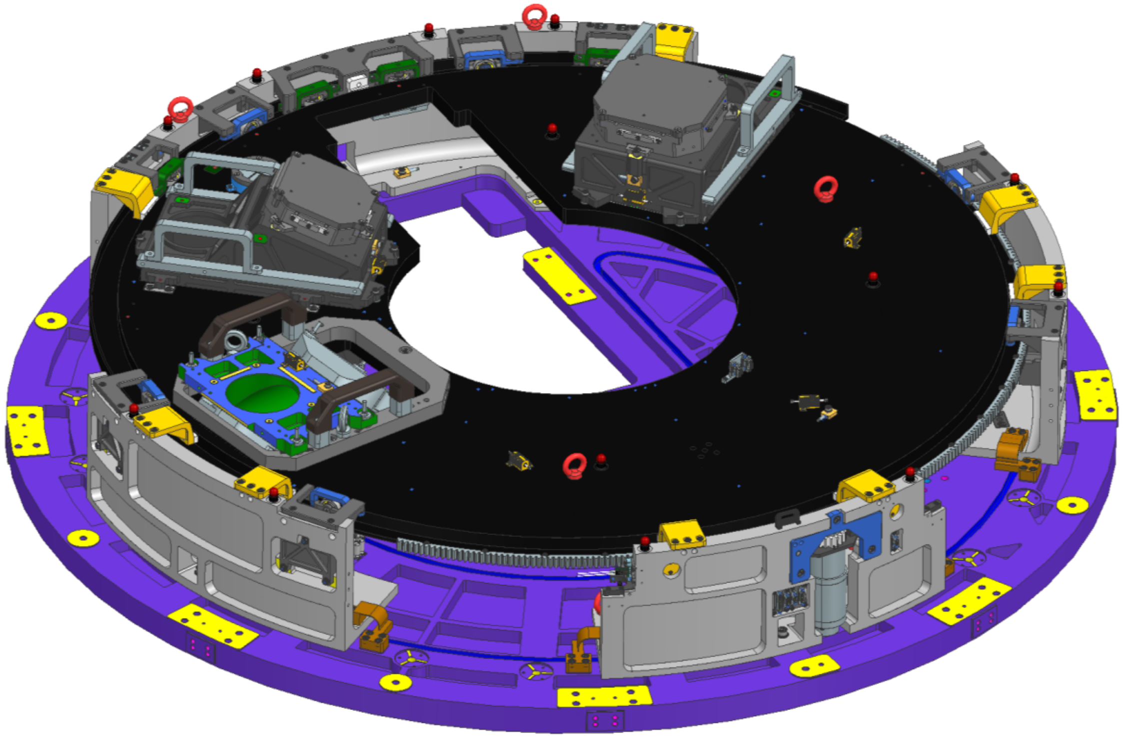

Neutrinos from colliding stellar winds: An analysis for η Carinae and γ^2 Velorum

Lang Bernhard

Institut für Astro- und Teilchenphysik, Universität Innsbruck

Diffusive Shock Acceleration

An incident particle with velocity v is accelerated by the Fermi I acceleration mechanism.

$$\frac{\Delta E}{E} \propto \frac{u_1 - u_2}{v}$$

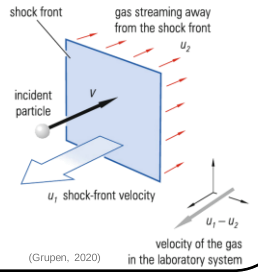

(Grupen, 2020)

Colliding wind binaries

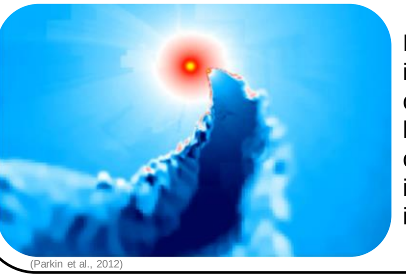

(Parkin et al., 2012)

Particles are accelerated in the bow-shaped wind collision region. Those high energy particles could produce ν while interacting with the interstellar medium.

Particles and neutrino events

Particle populations for electrons and protons are given by a powerlaw with exp. cutoff, where $\alpha \approx 2$ follows from DSA mechanism.

$$\phi = E_{\mathrm{tot}} \left(\frac{E}{1\,\mathrm{erg}}\right)^{-\alpha} \exp\left(\frac{E_{\mathrm{cut}}}{1\,\mathrm{TeV}}\right)^{\beta}$$

As for the detected ν events the effective area A_ν^{eff} of the detector, the differential neutrino flux as well as a visibility parameter ϵ_ν of the source are needed.

$$N_{\mathrm{ev}} = \epsilon_\nu\, t \int_{E_\nu^{th}} \mathrm{d}E_\nu \frac{\mathrm{d}N_\nu(E_\nu)}{\mathrm{d}E_\nu} A_\nu^{\mathrm{eff}}$$

Neutrino predictions in KM3NeT

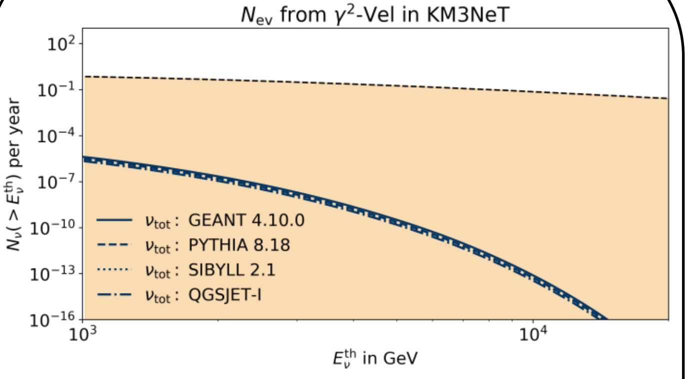

The predicted neutrino interactions N_{ev} in KM3NeT are unitarily below the atmospheric background (shaded area) for all considered models and systems.

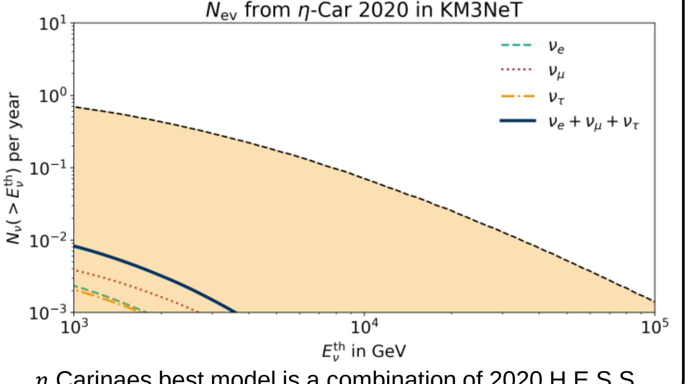

η Carinaes best model is a combination of 2020 H.E.S.S. data and two proton populations. It would be necessary to integrate over 100 yrs to detect a single source-related ν.

SEDs and corresponding models

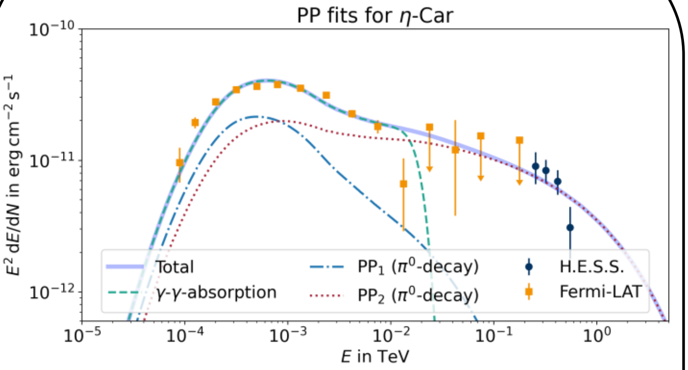

Multi wavelength data from H.E.S.S. (2014 and 2020), Fermi-LAT and NuSTAR is used to fit the SED for η Carinae. Purely hadronic, lepto-hadronic and costrained lepto-hadronic models are used.

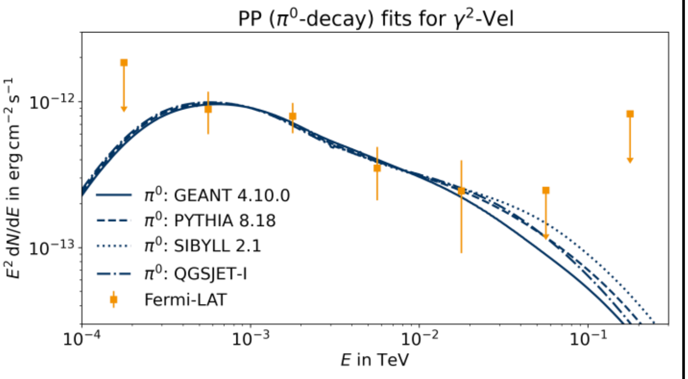

For γ^2 Velorum observational data by Fermi-LAT with a single proton population and four different neutrino cross section parametrizations are used.

References

Grupen, C. (2020). *Astroparticle Physics* (2nd ed.). Springer International Publishing AG

Parkin, E. R., & Gosset, E. (2012, October 12). Accessed on 2024, May 06. *Colliding winds at WR 22*. ESA - Colliding winds at WR 22. https://www.esa.int/ESA_Multimedia/Videos/2012/10/Colliding_winds_at_WR_22

Machine Learning using Beam Loss Monitors for Diamond-II

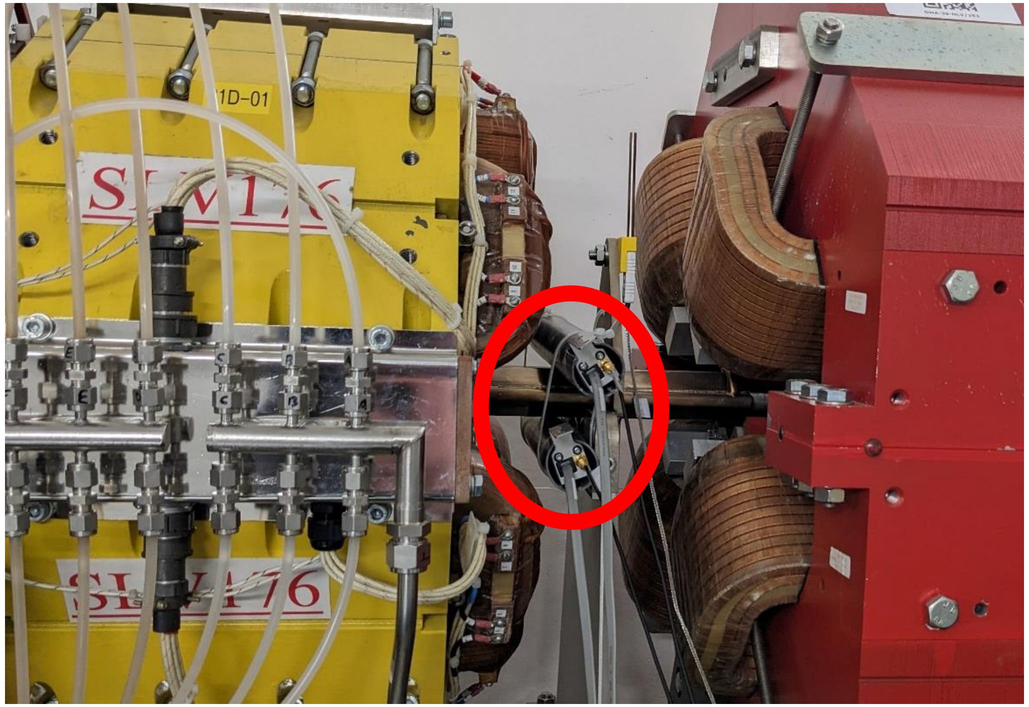

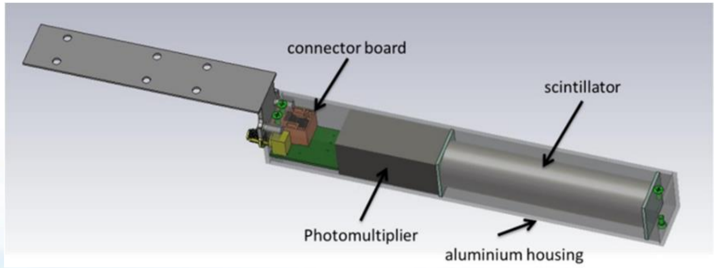

Can Machine Learning techniques help us understand and reduce beam losses in an ever-changing complex machine?

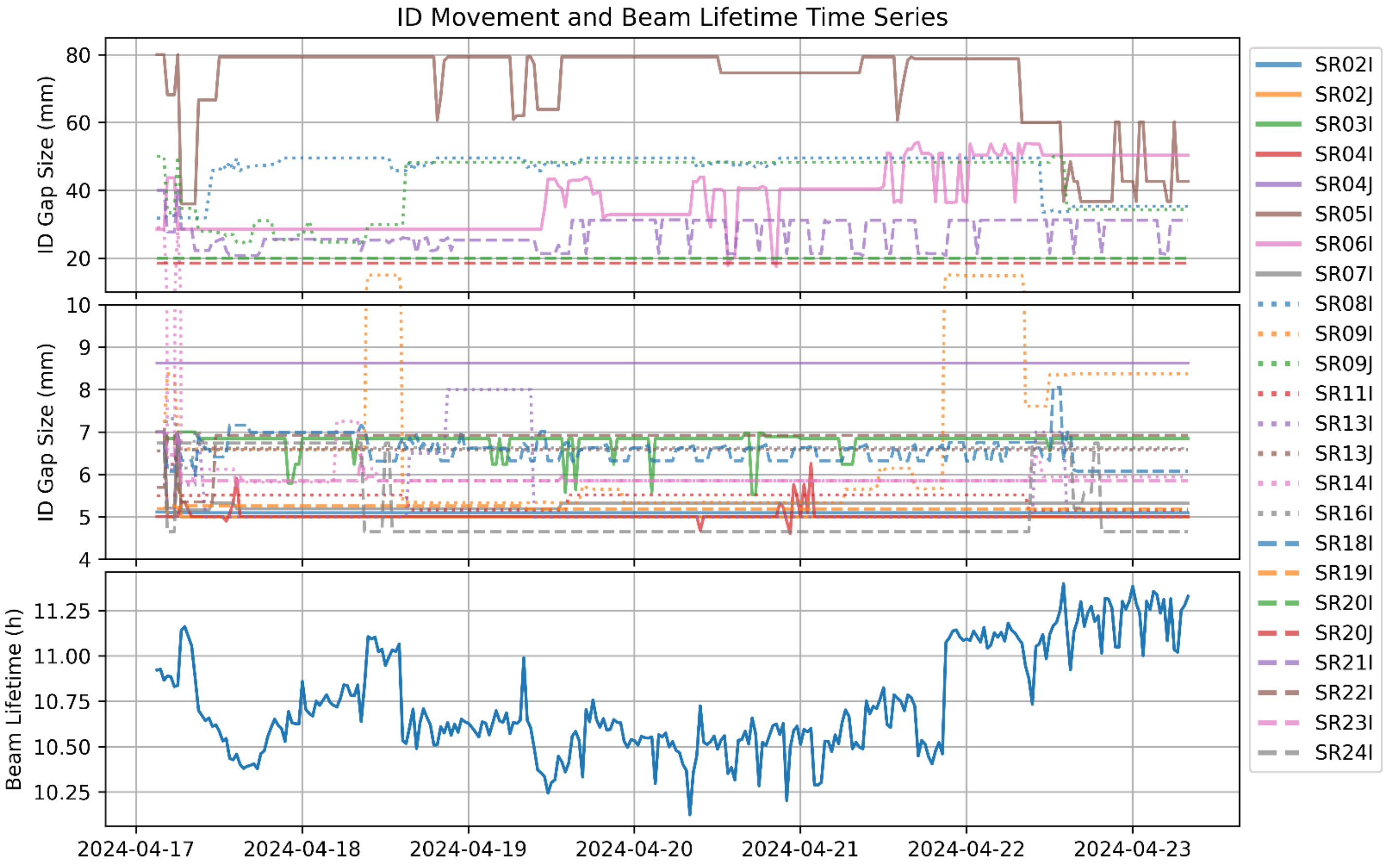

Corey Lehmann

John Adams Institute for Accelerator Science
UNIVERSITY OF OXFORD
diamond

Laser ultrasound for the *in-situ* inspection of plasma-facing components

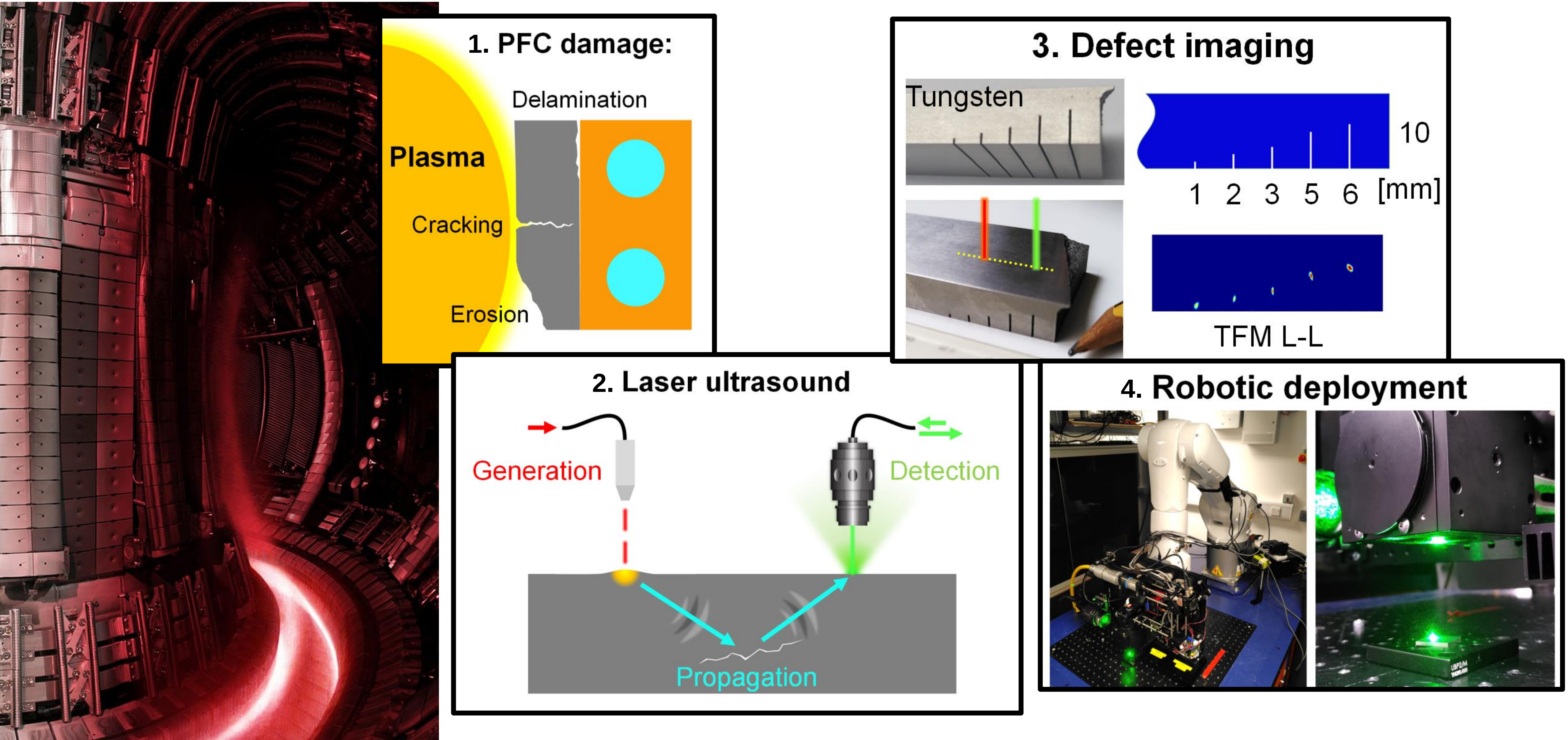

Superconducting Microstrip Resonators

Karlsruhe Institute of Technology

- Polycrystalline diamond (tanδ~**10^{-5}**) windows losses are characterized with Fabry- Perot resonators (Q~ **10^4 - 10^5**).
- Future increase in ECRH power will require improved tanδ (**~10^{-6}**) to avoid window overheating
- **Higher Q resonators needed for increased resolution**.
- Superconducting lumped elements (LE) microstrip resonators show Q factors routinely above 10^6

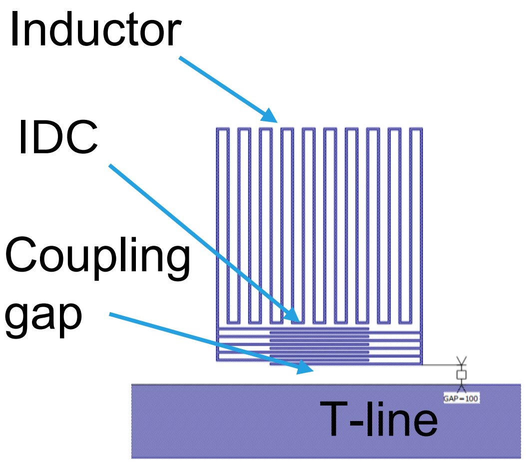

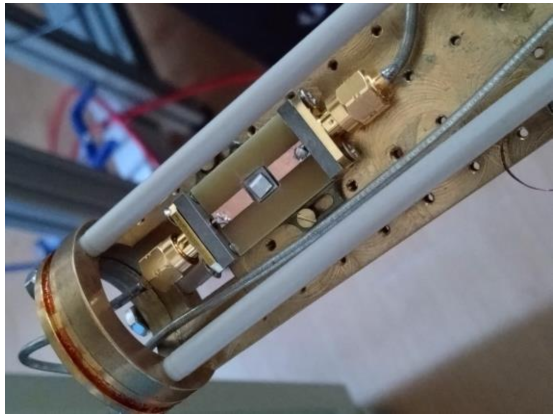

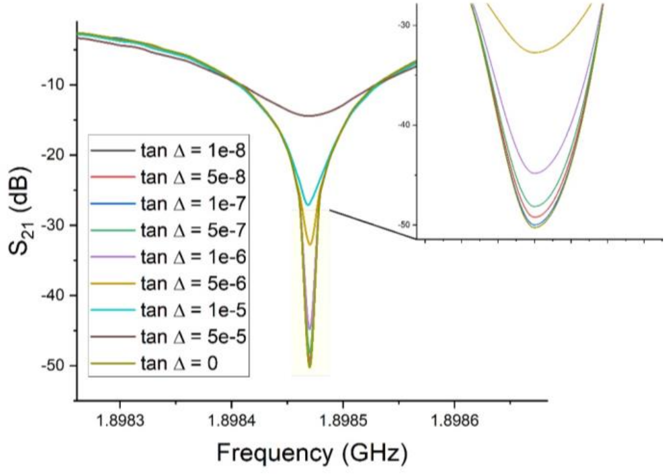

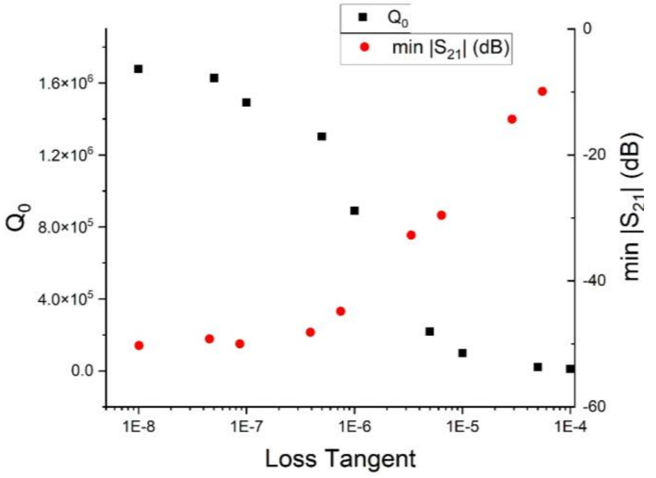

- Resonance curve shape linked to substrate losses (higher losses → shallower and wider resonances = lower Q)

Mechanical Design of a Small Pixel PNCCD Camera

Jonas Mügge
*Max Planck Institute for Extraterrestrial Physics, Garching, Germany

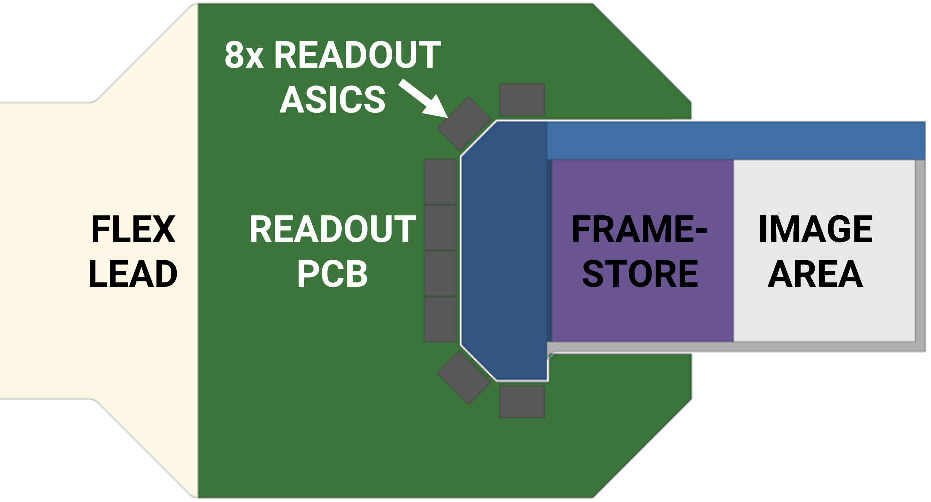

Goals:

The Max Planck Halbleiterlabor (HLL), in conjunction with the MPE, plan to produce CCDs (Charge Coupled Devices) with small pixel sizes in large arrays. These show excellent promise to match X-ray optics of the future.

Challenges:

The high number of readout ASICs necessitates splitting the CCD sensors and readout electronics into two separate thermal paths.

However, these two elements must be connected via fragile wire bonds. An ideal thermal suspension must exhibit a high stiffness, and a low thermal conductivity, while satisfying all other system requirements.

$$\uparrow K, \downarrow k$$

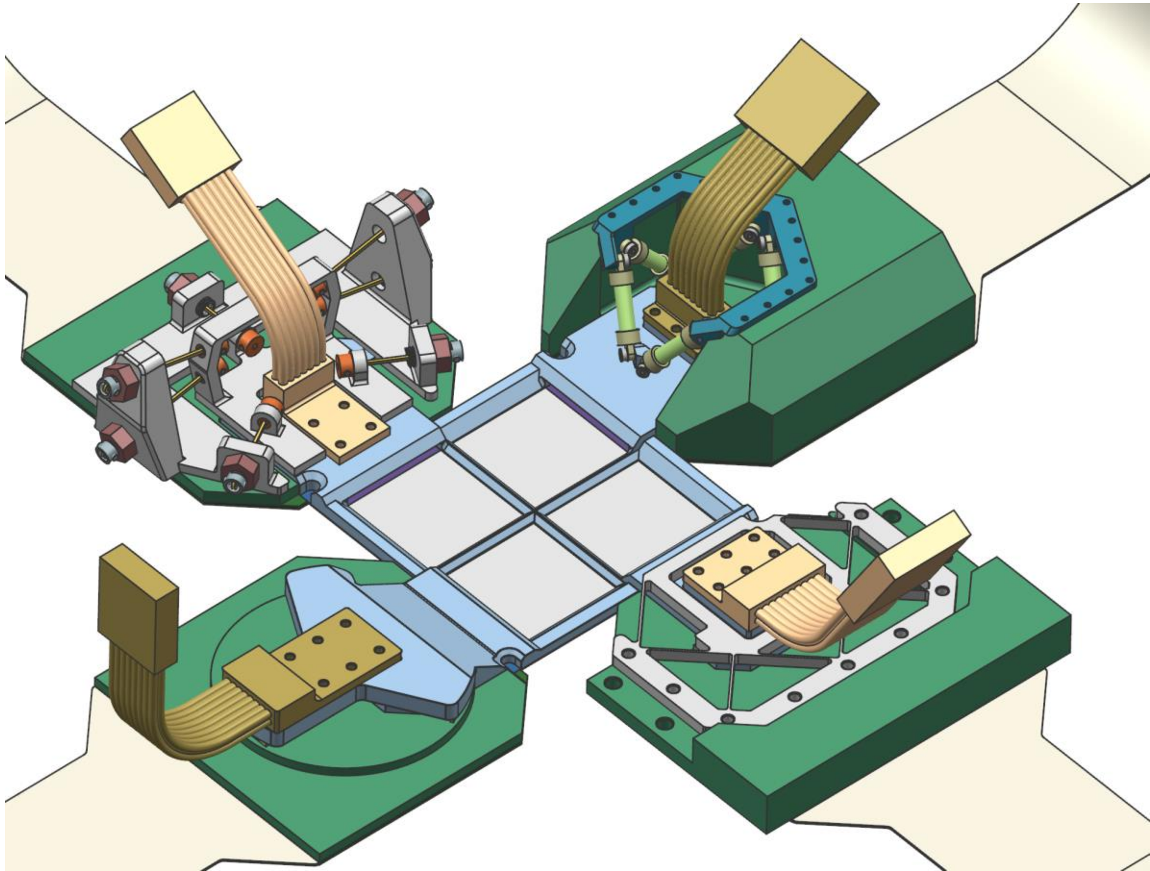

3D FIELD MAPPING SYSTEM FOR EXPERIMENTAL MAGNETS

Lukas Messner

EP-DT
Detector Technologies

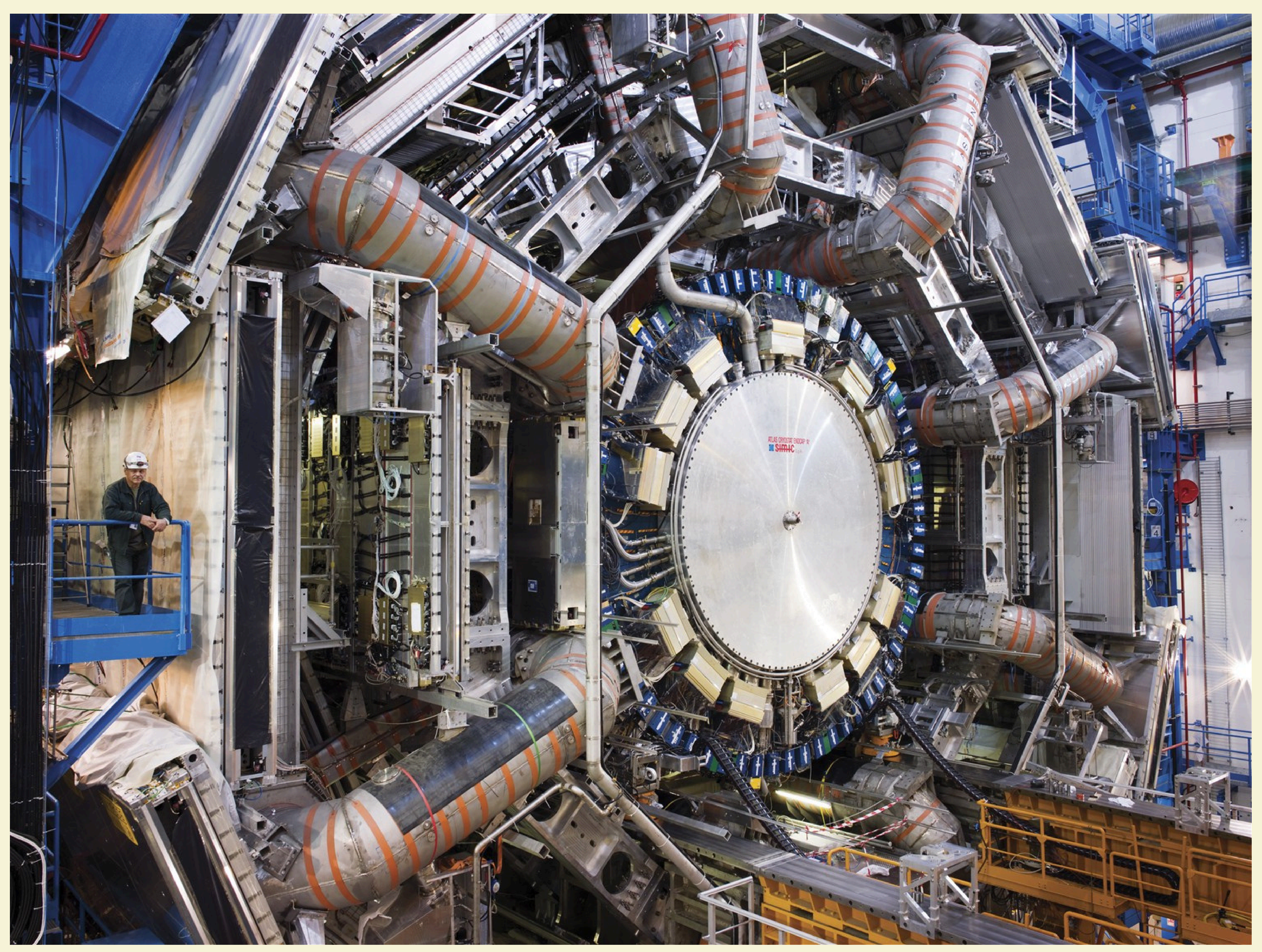

MAGNETIC FIELD MAPPING OF HIGH ENERGY PARTICLE PHYSICS EXPERIMENTS

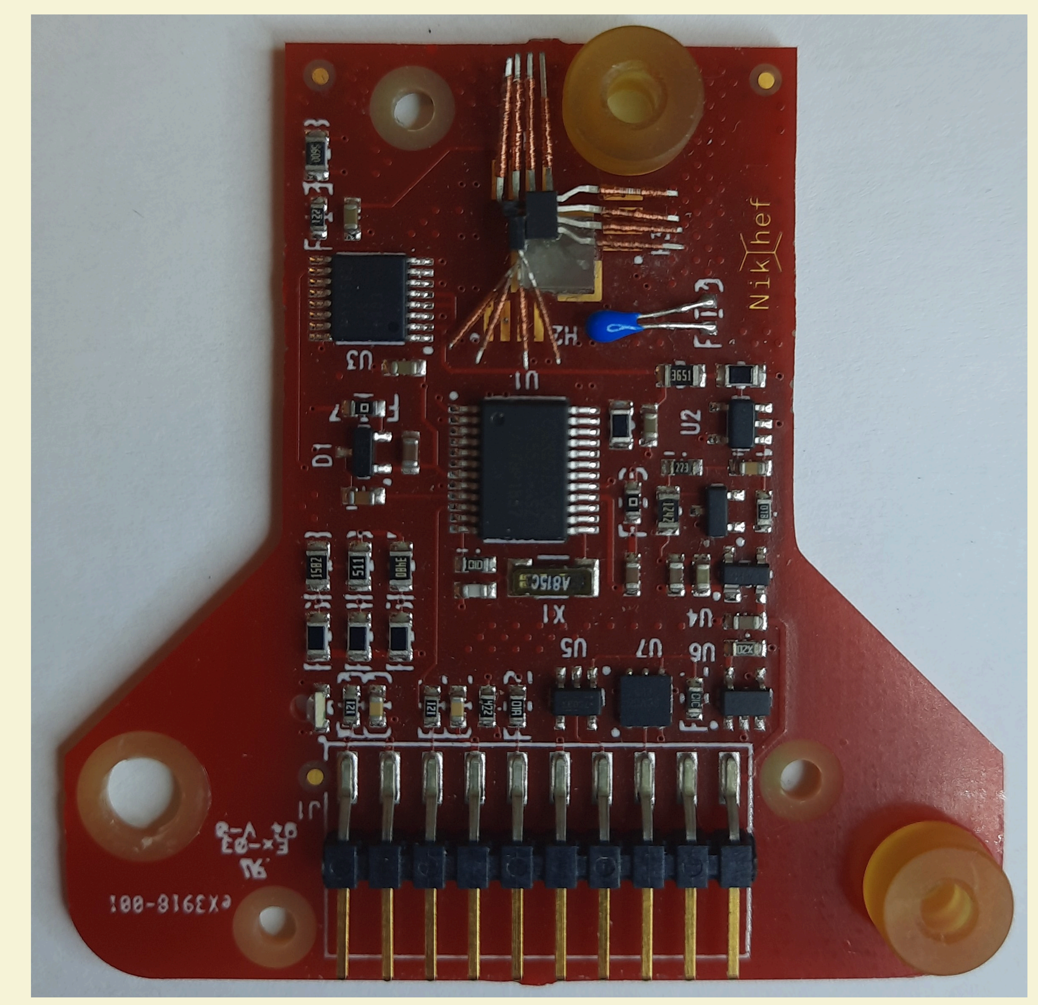

3D HALL PROBE MAGNETIC FIELD MEASUREMENT CARD

CALIBRATION PROCEDURE FOR 3D HALL PROBES

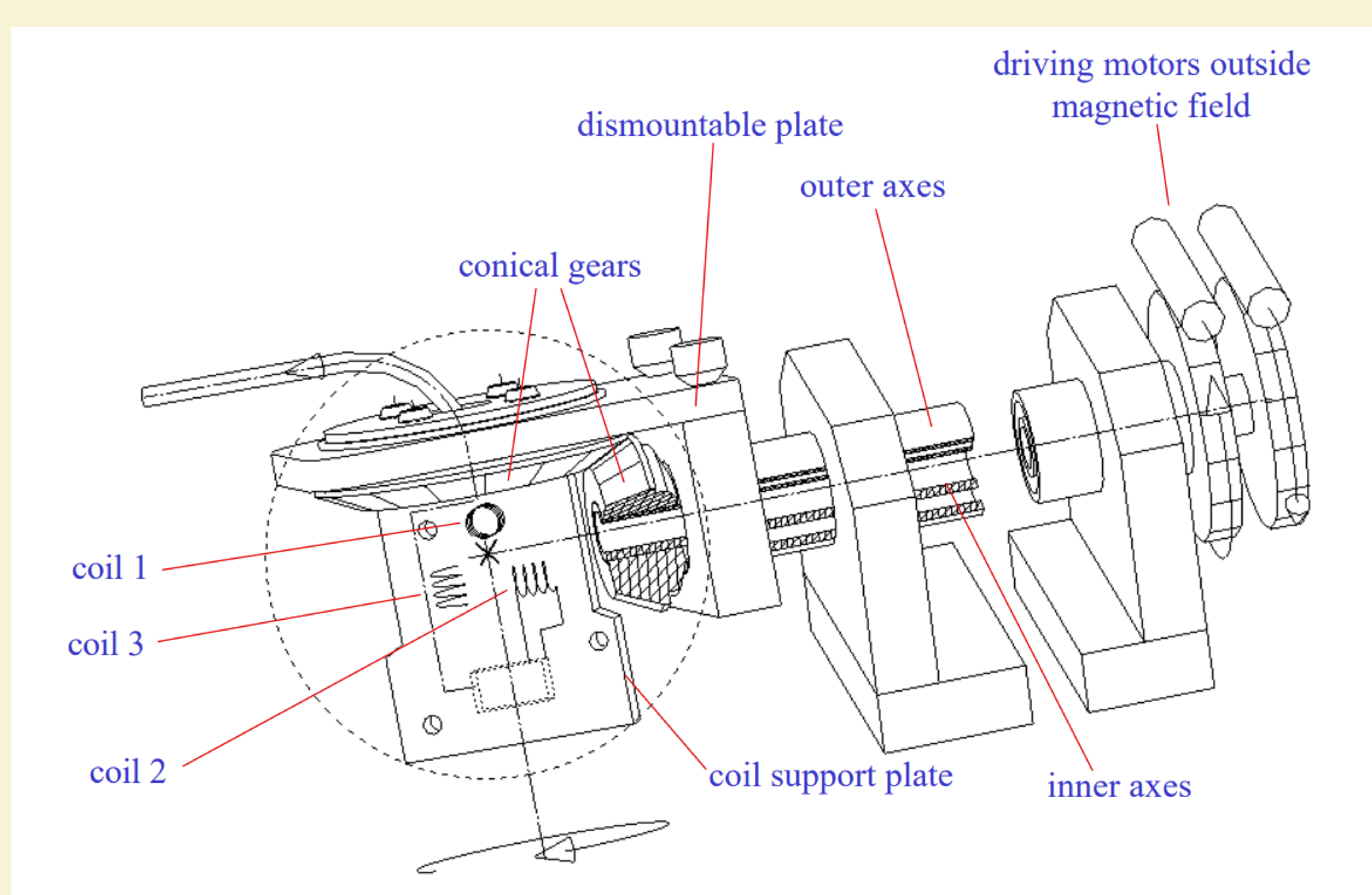

MAGNETIC FIELD MAPPING SYSTEM

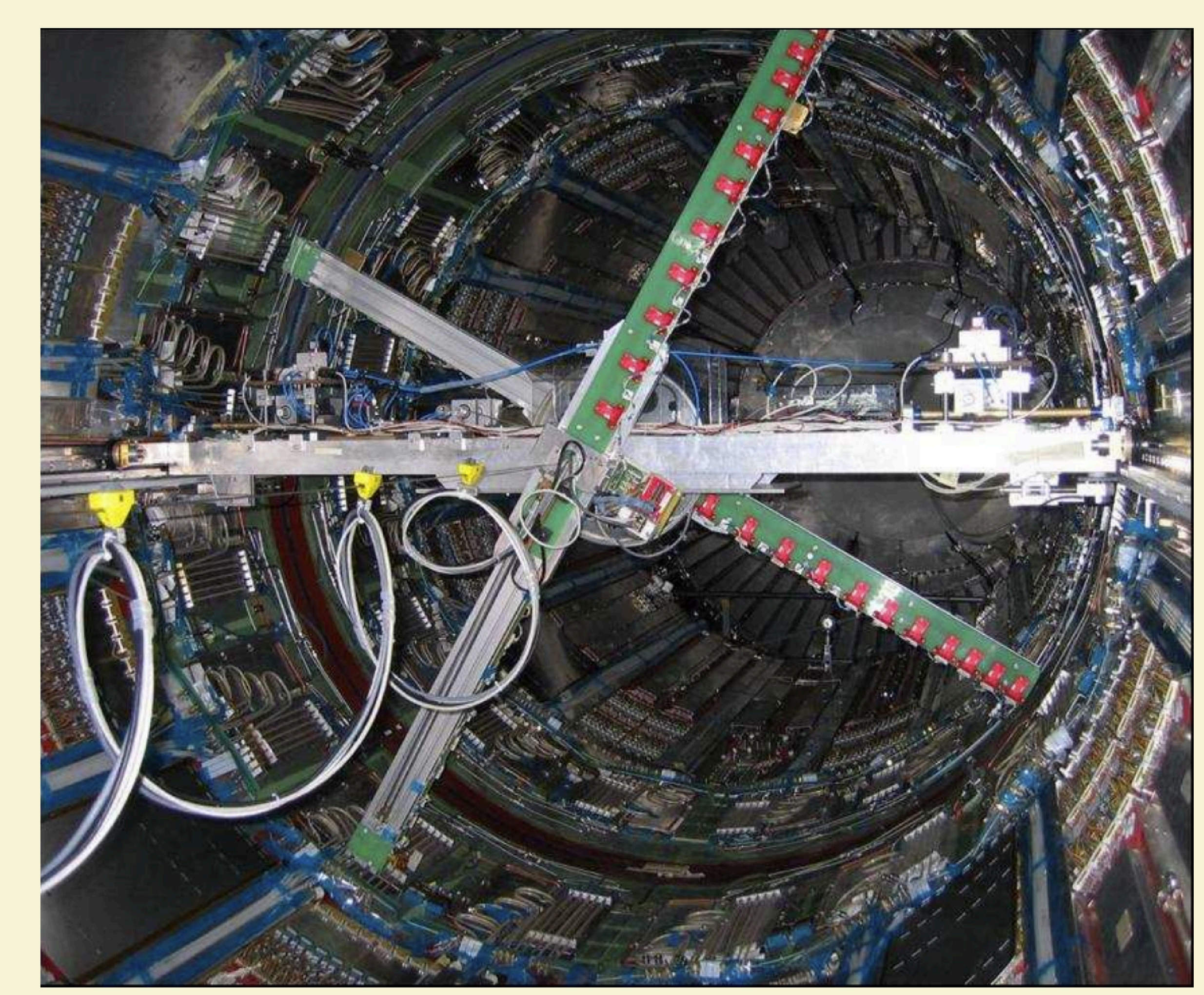

Inner Tracking System 3

Detector Overview

- Wafer-scale MAPS ASICs
- Fabricated with stitching
- All electrical signals and power routed on-chip
- Out-chip signal and power placed on the edges of the chip
- Ultra-thin and bendable: 50 µm

Key benefits

- Extremely lightweight
  - Material budget: 0.35% X_0 => 0.05% X_0
- Closer to the interaction point
  - Radial position: 24 mm => 19 mm

Tasks/Topics

- DFM low leakage standard cell
- ITS3 behavioral model
- ITS3 on-chip readout architecture

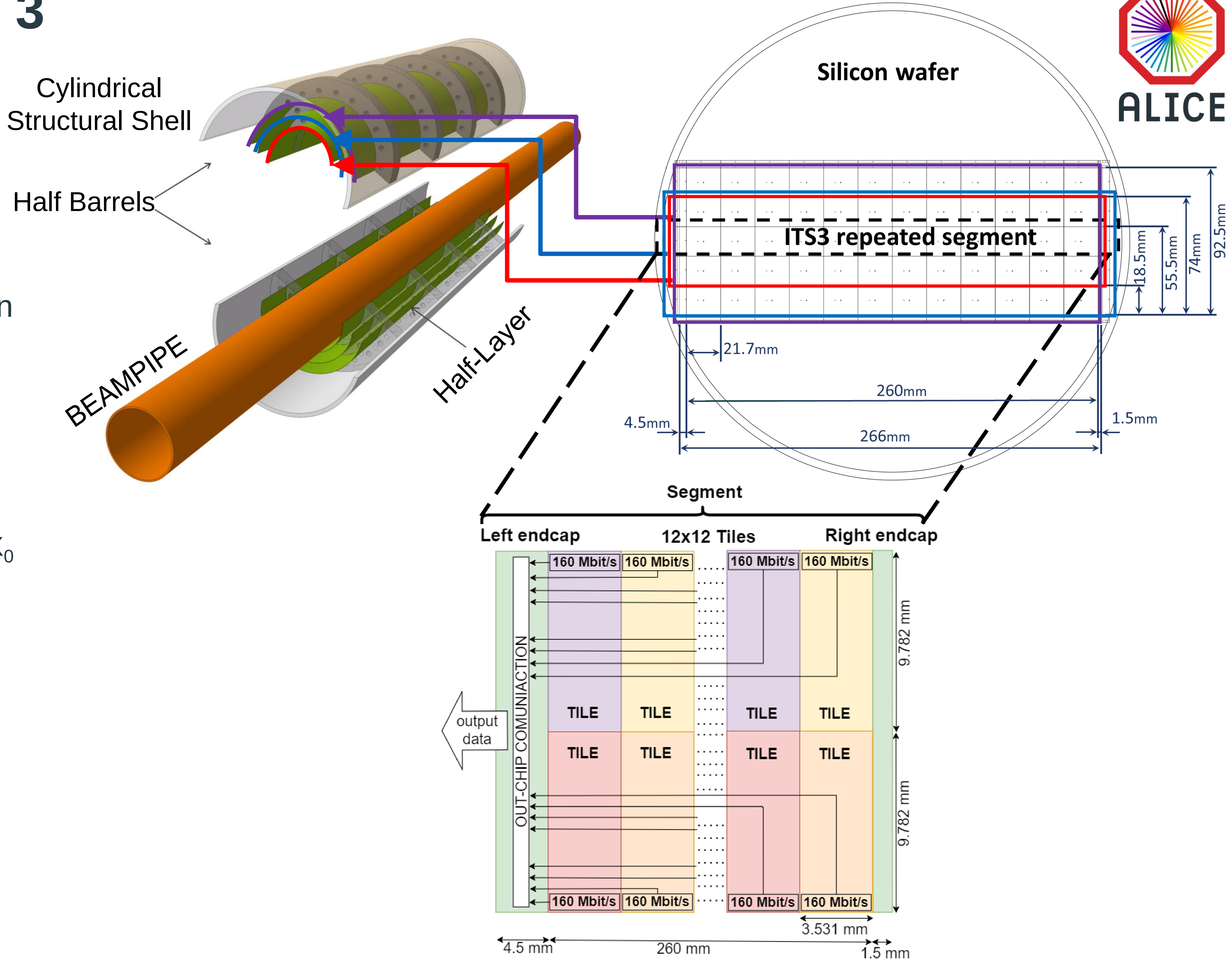

Me – In a Nutshell

My name is **Sara**, I am a **Nuclear Engineering** master student at **Politecnico di Milano**.
My major interests in this field concern Reactor Physics and Nuclear Materials.

POLITECNICO
MILANO 1863
DIPARTIMENTO DI ENERGIA

WIN
WOMEN IN NUCLEAR ITALY

For a few months now, I've been part of the association '**Women in Nuclear**' - Italy, with the aim of encouraging more women to pursue a nuclear career and creating a more inclusive environment.

My mission is also to ensure that there's **no misinformation** about nuclear energy, across all age groups.
Together we can WIN!

Let's build a brighter future! 🌞

Inspo: Kurzgesagt - In a Nutshell

Thermal design of ATHENA Wide Field Imager (WFI)

What?

Camera Head Thermal Design of Wide Field Imager (WFI)

Why?

Operating temperature of the detector and radiator area minimization

How?

Separate cooling chains for the detector and front-end electronics

Challenge?

Reduced radiator area allocation after reformulation of ATHENA project

Solution:

Optimized thermal design with focus on parasitic heat flow reduction

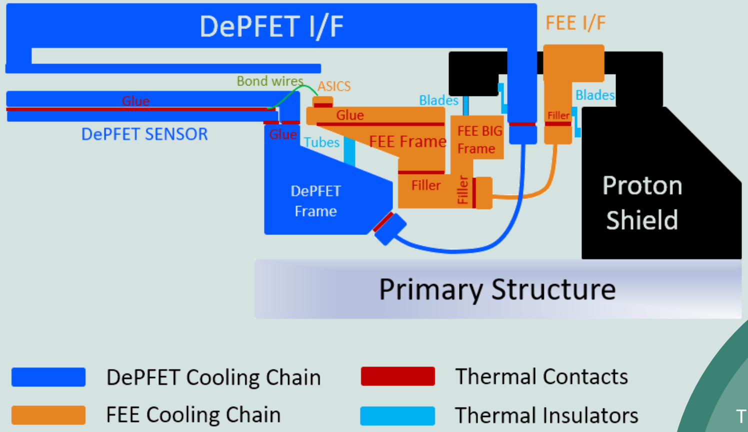

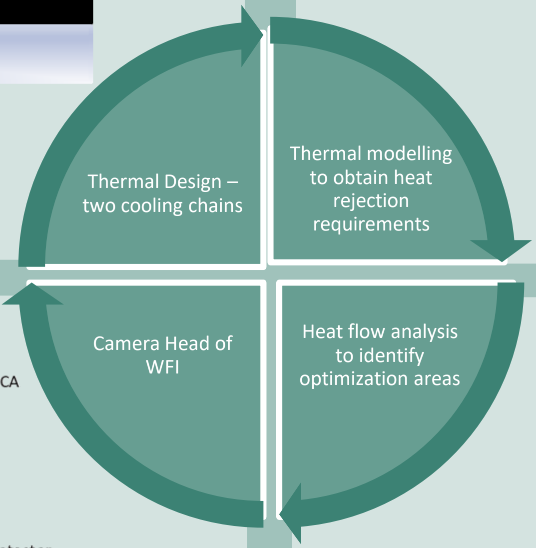

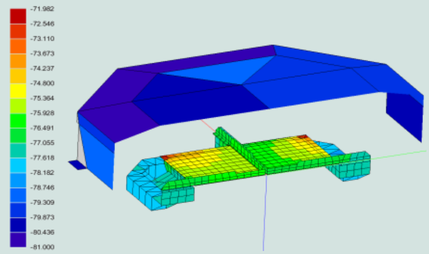

Interface	Interface temperature	Heat load (with design margin of 1.2)
DEPFET thermal Interface	BoL - 193 K, EoL - 173 K	BoL and EoL - 31 W
FEE thermal interface	BoL - 260 K, EoL - 240 K	Bol - 32 W, EoL - 37 W

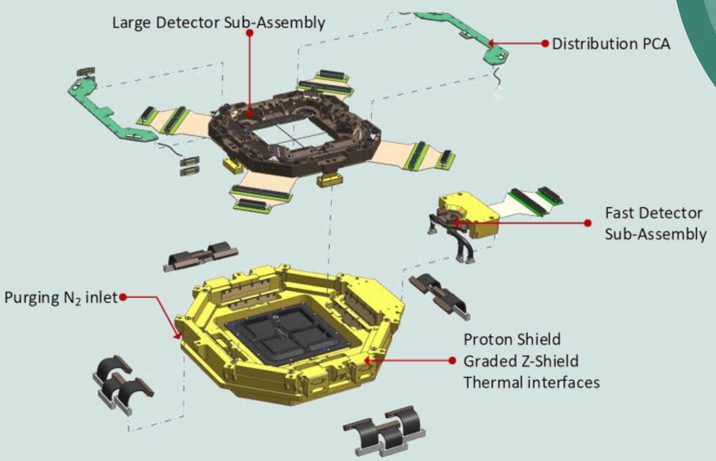

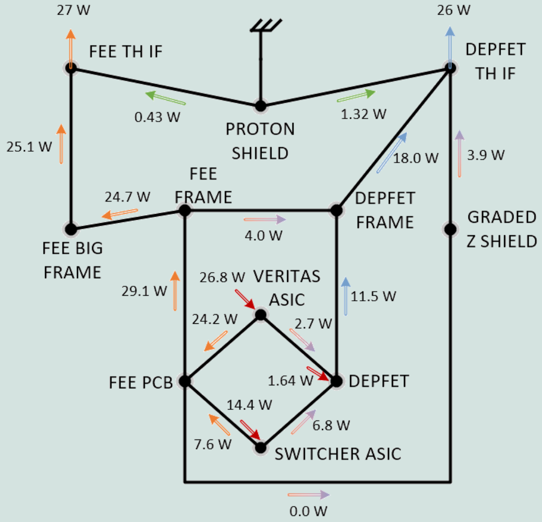

Anirudh Mukund Saraf, EIROforum School on Instrumentation (ESI), May 13th to 17th 2024

Augusto Sciuccati

Annihilation-Gamma based Diagnostics for Magnetically Confined Electron–Positron Pair Plasma

Jens von der Linden - Max Planck Institute for Plasma Physics

Expected annihilation in dipole confined pair plasma

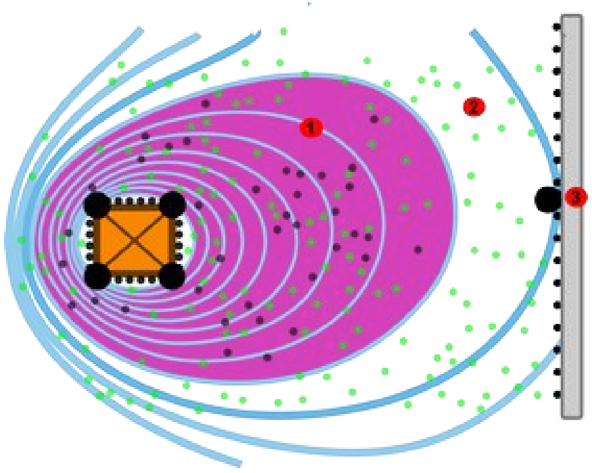

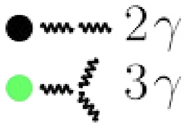

1. Direct annihilation and decay of positronium formed by atomic processes

2. Drift and decay of long-lived Ortho-Ps in vacuum

3. Plasma transport to wall and Ps drift to wall

Test gamma detector-array in recent positron confinement experiments

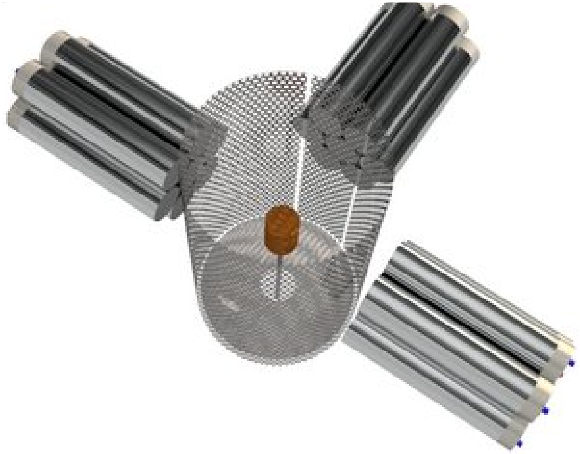

Toroidal expansion of a positron bunch

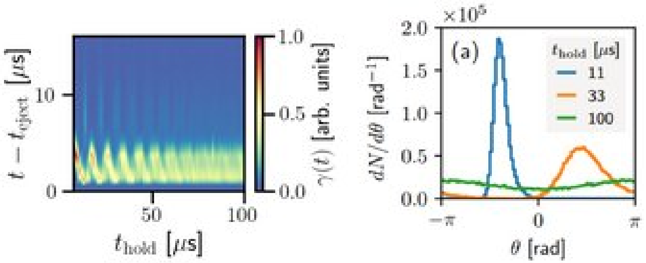

Cooling through inelastic collisions

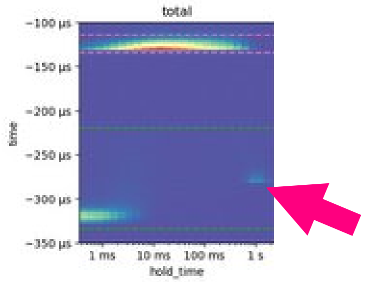

Lifetime

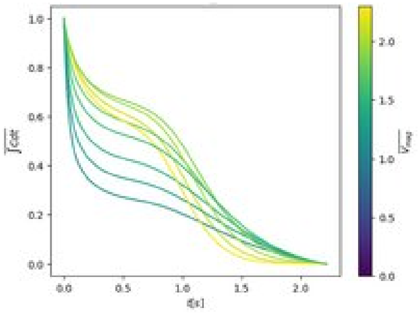

Positronium formation

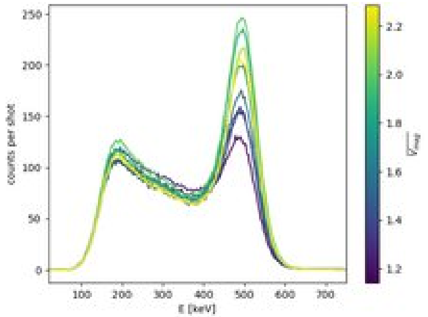

FREDERIK WOHLLEBEN: GAMMA RAY ASTRONOMY

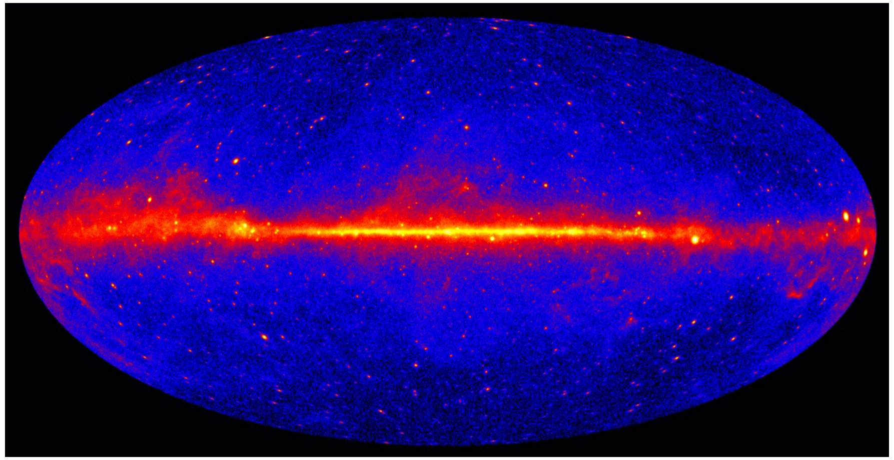

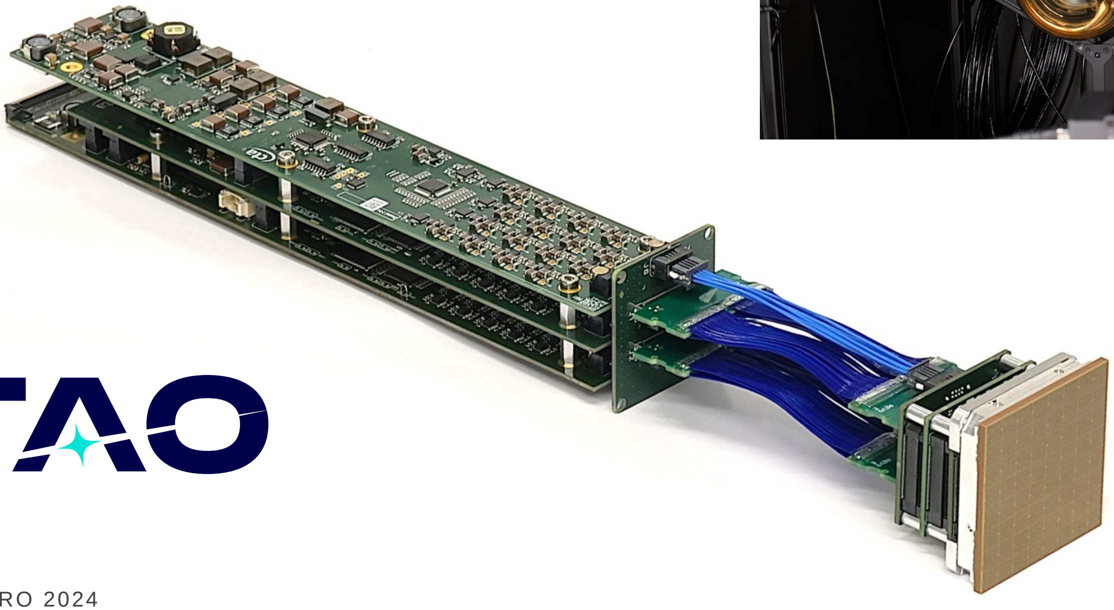

CTAO

SWGO
The Southern Wide-field Gamma-ray Observatory

Reconstruction and Interpretation of POD Modes of Heat Flux on the W7-X Divertors

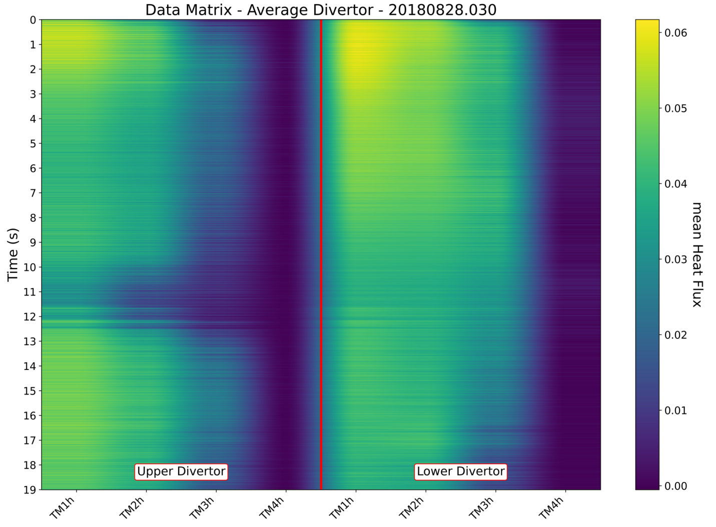

- **Spatial-Temporal Data Matrix**: Illustrates heat flux variations across W7-X divertor surfaces, enabling a detailed observation of fluctuation patterns.

- **Primary POD Mode Highlights**: Identifies and emphasises the key modes encapsulating the majority of data variance, underscoring their significance in understanding plasma dynamics.

- **Correlation Insights**: The direct correlations between dominant POD modes and crucial plasma parameters such as diamagnetic power or the bootstrap current, provide insights into their physical relevance.

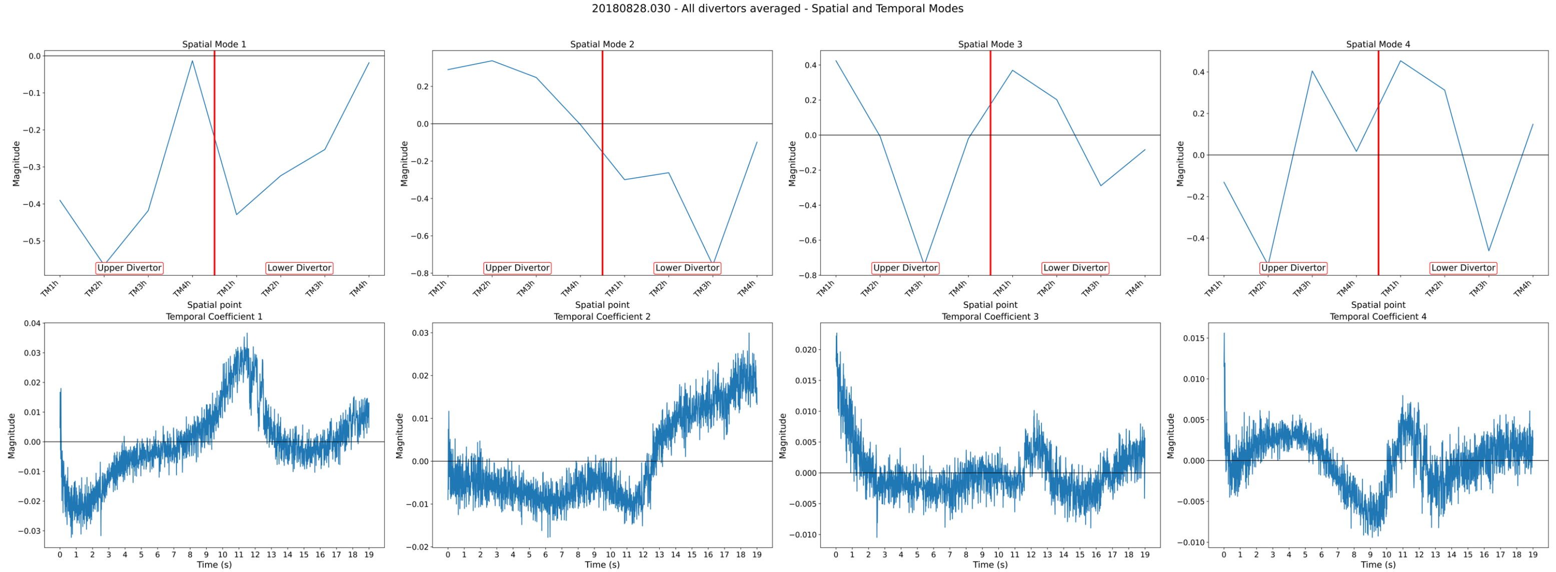

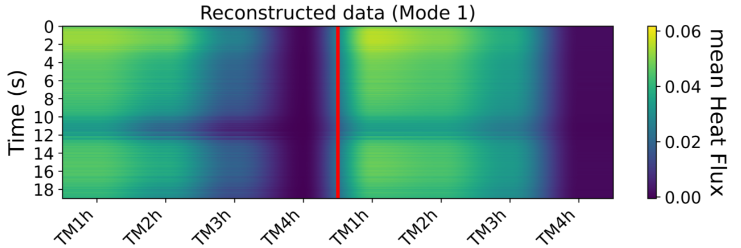

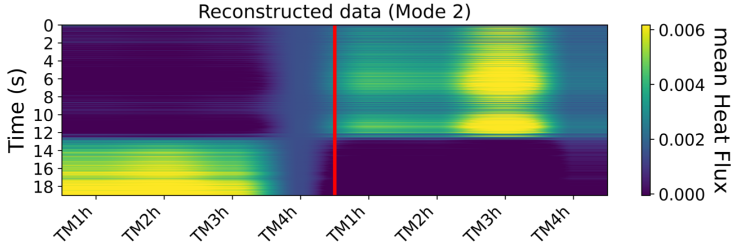

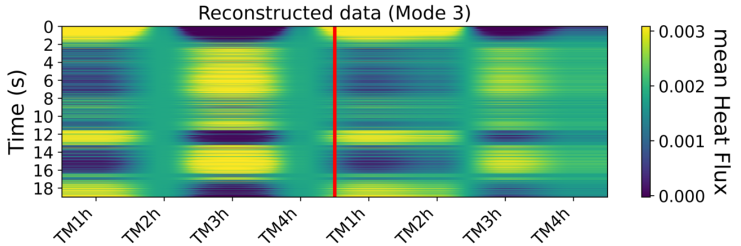

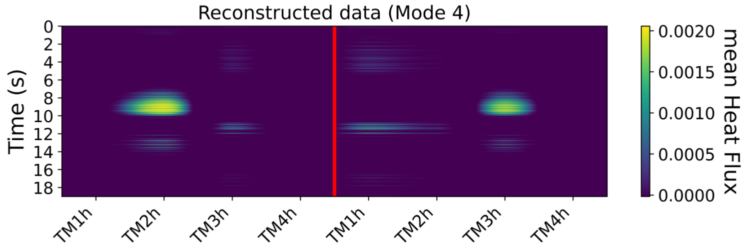

Design proposal for the DEMO Electron Cyclotron ex-vessel waveguide system

Enhancing remote maintainability in DEMO-class tokamaks

Introduction

- In DEMO, shutdown dose rates in the port cell are expected to be too high for human hands-on intervention (>10 µSv/h)

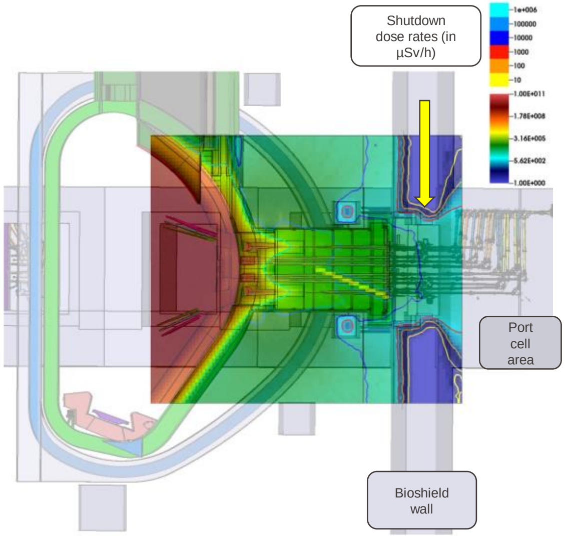

Figure 1: DEMO reactor overlay with shutdown dose rate analysis

Objectives

- Enhance remote maintainability
- Redefine structural dynamics to streamline the design

Design proposal

- Transitioning from individually double sealed to sealless waveguides within a vacuum casing
- Reconfigure the first confinement system to move in unison with the vacuum vessel

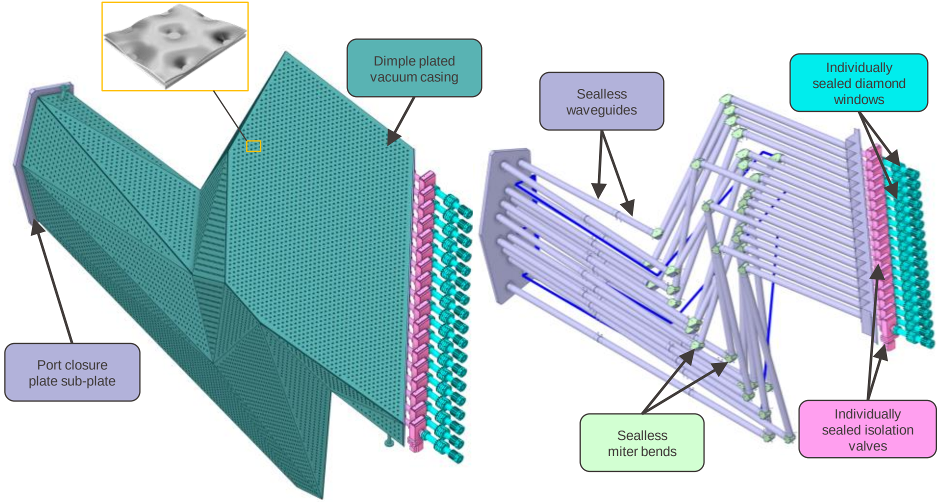

Figure 2: First confinement ex-vessel waveguide system

Conclusion

- Findings for a pre-assembled casing approach are promising, improving maintenance efficiency and reliability
- Further studies are required to assess if the design fits all of the requirements

Fiber Fabry Perot for wavelength calibration

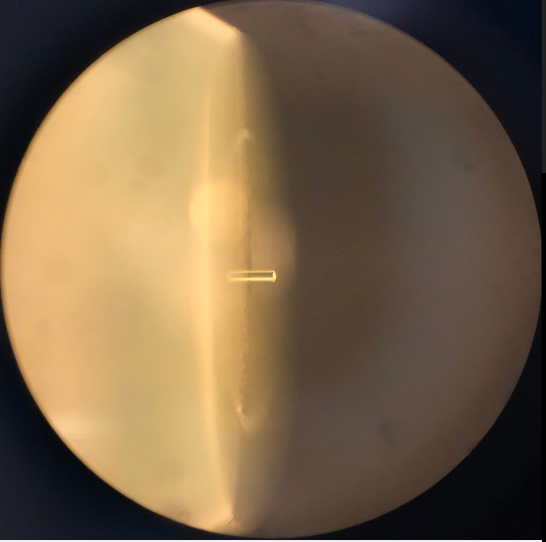

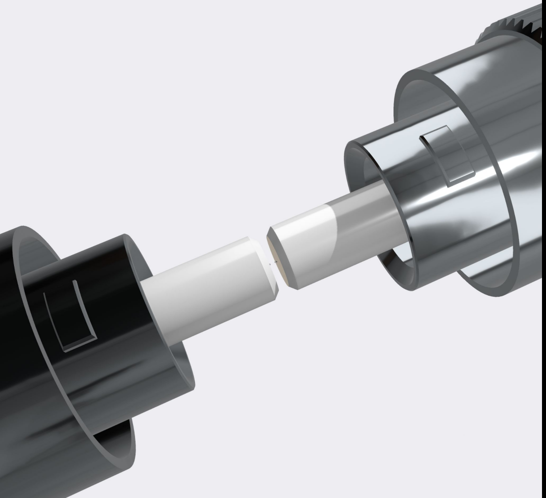

Sebastian Bok, MPIA Heidelberg

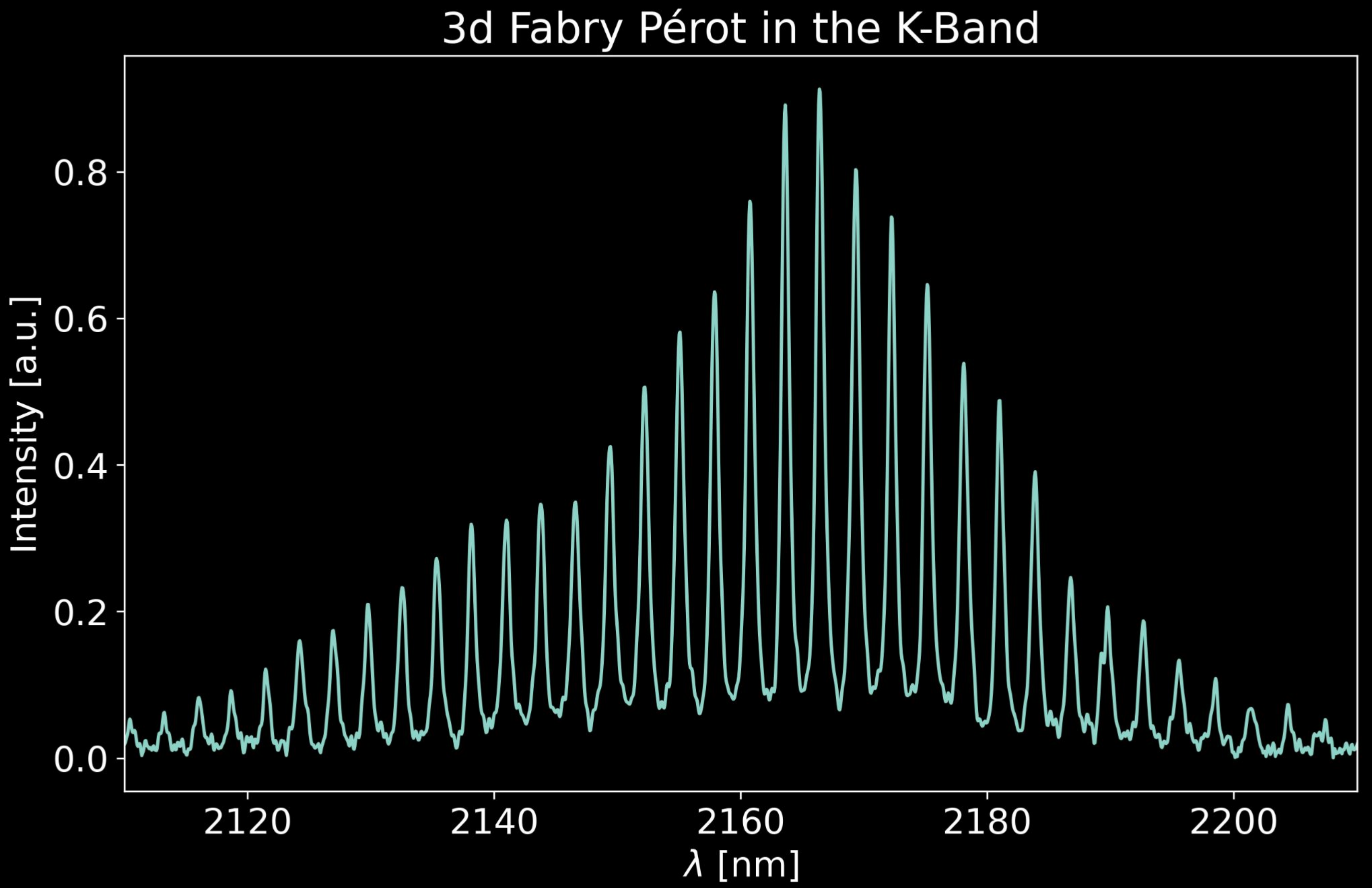

MICADO Data Reduction Pipeline

Yixian Cao and the MICADO Consortium

Max-Planck Institute for Extraterrestrial Physics

Introduction

The MICADO data reduction pipeline is designed to provide data products ready for scientific analysis and instrument health monitoring from the raw data produced by the instrument. The pipeline supports all the four observation modes offered by MICADO: standard imaging, astrometric imaging, high contrast imaging, and slit spectroscopy. The pipeline software will be implemented in the ESO software framework, using the Common Pipeline Library and the High-level Data Reduction Library developed by ESO. For a successful implementation, the pipeline should timely and robustly produce processed data that meets quality requirements of each observation mode. To achieve this goal, simulated data and instrument test data when applicable will be used for the pipeline testing.

Top-level Requirements

MICADO Capabilities

- Imaging
  - 0.8-2.4μm with 30 broad/narrow filters
  - 1.5 & 4mas pixels for 19 & 51" FoV
  - Similar sensitivity to JWST, and 6× better resolution
- Astrometric imaging
  - 50μas precision anywhere in the field
  - 10μas/yr = 5km/s at 100 kpc after only a few years
- High contrast imaging
  - Focal & pupil plane coronagraphs
  - Angular differential imaging
  - Small inner working angle
- Slit spectroscopy
  - For compact sources
  - fixed configuration for 0.84-1.48μm & 1.45-2.46μm
  - R ~ 20,000 for point sources (R ~ 10,000 across slit)

Science Drivers

- Galaxy Formation and Evolution
  - Resolved stellar populations, SFHs
  - Internal structure
  - QSO host galaxies
- Massive Black Holes
  - Galactic Center
  - IMBHs
  - BH – galaxy co-evolution
  - Seed BHs
- Exoplanets (atmospheres)
  - At small orbital separations (~1AU) around nearby stars (< 20 pc)
  - At larger separations (>10AU) around more distant stars (> 100 pc)
  - Circumstellar disks

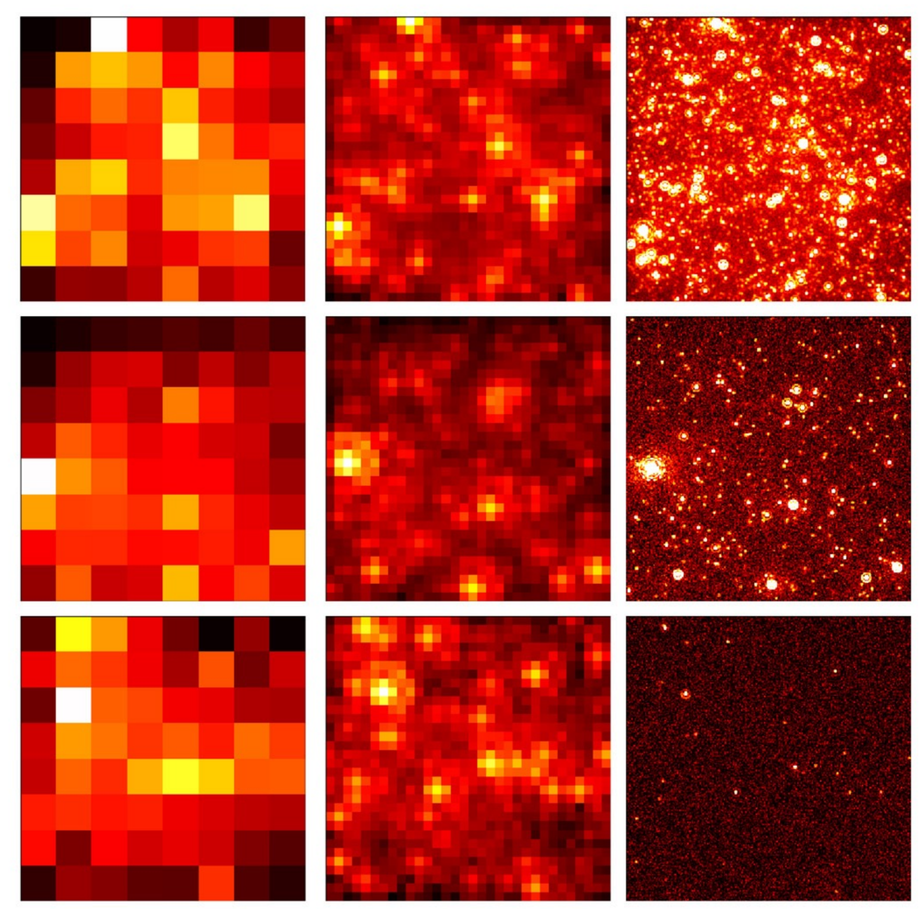

MICADO Pipeline Conceptual Overview

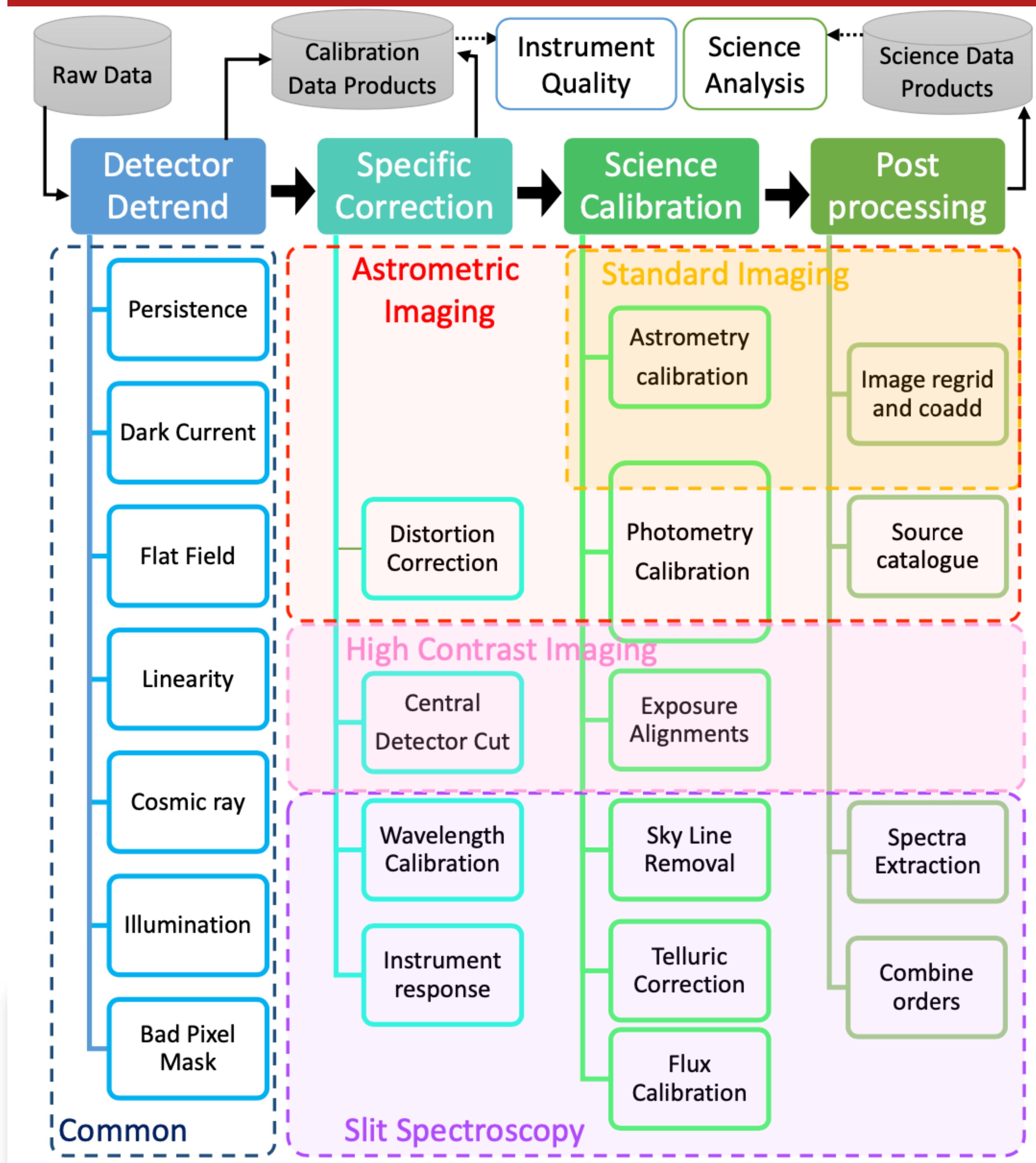

The pipeline processes the **raw data** into **calibration and science data products.**

In the *Left* figure:

- Arrows: data flow through the processing
- Rectangles: main steps in the pipeline
- Blue shaded box: the detector detrend steps; these are commonly used in all the four observing modes.
- Red, yellow, magenta and purple shaded boxes: steps for data reduction of astrometric imaging mode, standard imaging mode, high contrast imaging mode, and slit spectroscopy mode respectively.
- Dotted lines: procedures beyond the scope of the pipeline

Implementation in the ESO software framework

Implantation and development

- The processing cascade describes the workflows and relations between input/output data for each instrument mode
- Each workflow includes several recipes
- Each recipe is implemented using the Common Pipeline Library (CPL) plugin interface, so it is a pluggable module to ESO's various front-ends
- Utilize the Common Pipeline Library (CPL) and the High-level Data Reduction Library (HDRL)

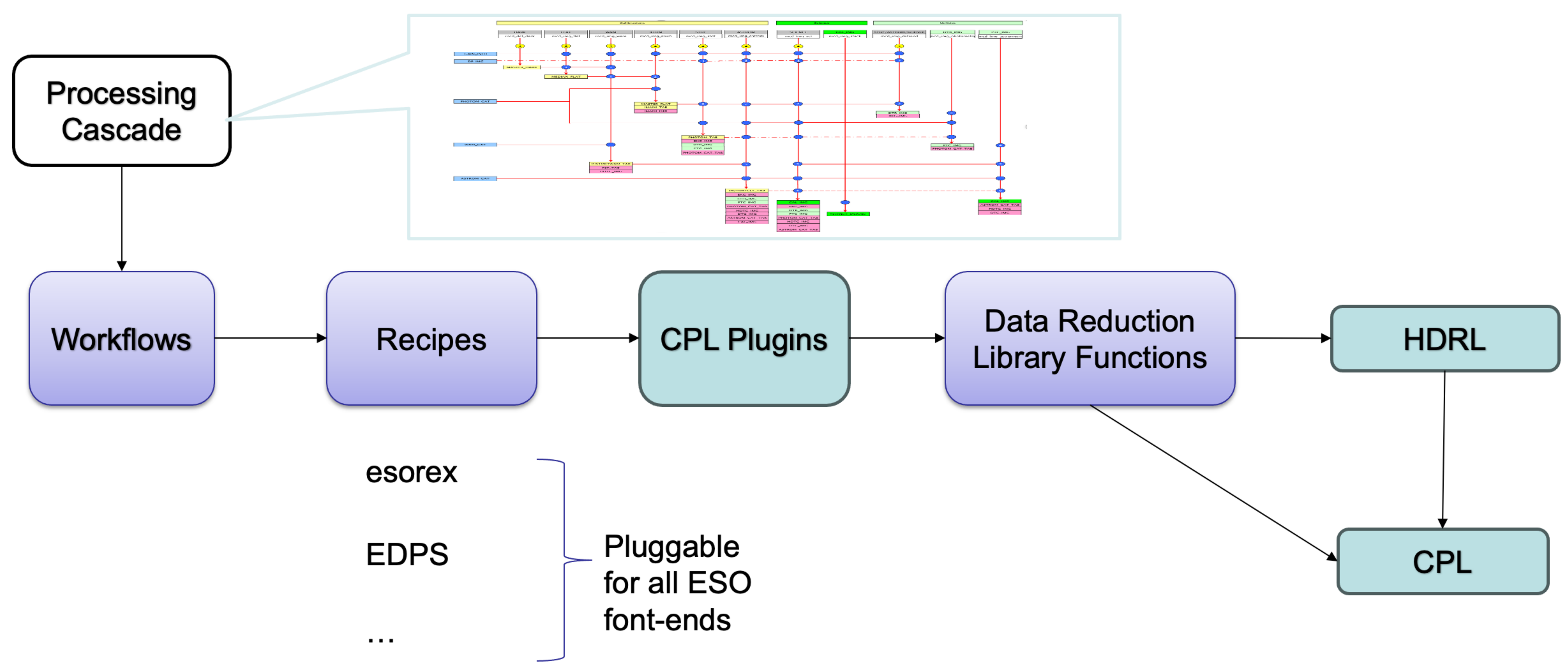

References

- Davies, R., Alves, J., Clénet, Y., et al. 2018, SPIE, 10702, 107021S. doi:10.1117/12.231148
- Davies, R., Schubert, J., Hartl, M., et al. 2016, SPIE, 9908, 99081Z. doi:10.1117/12.2233047

Contact

Yixian Cao (ycao@mpe.mpg.de)

Clusterization for photon hit reconstruction in iLGAD sensors

- iLGADs sensors have a gain layer for signal amplification, enabling soft X-ray applications (RIXS).
- Prototypes developed by FBK (sensors) & PSI (JUNGFRAU ASICS and readout board).
- With elongated pixels (225 x 25μm²) there is significant charge sharing in one dimension.
- Clusterization methods are essential to reconstruct photon hits:
  - Charge shared across cluster is summed and attributed to the central pixel.
  - A threshold based on pixel noise is applied to discriminate between noise and photon signal.
- Additionally, reconstruction methods (e.g., eta-function) can be used to achieve subpixel resolution.

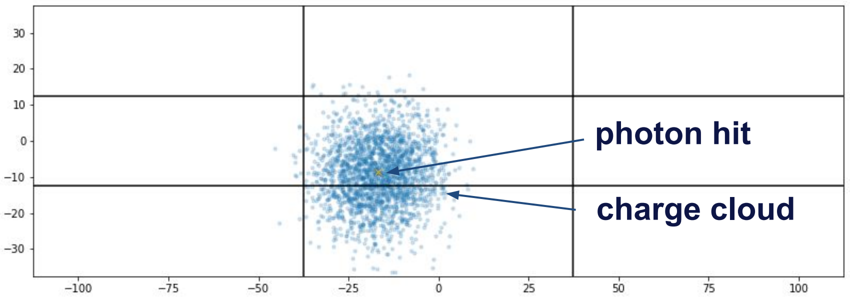

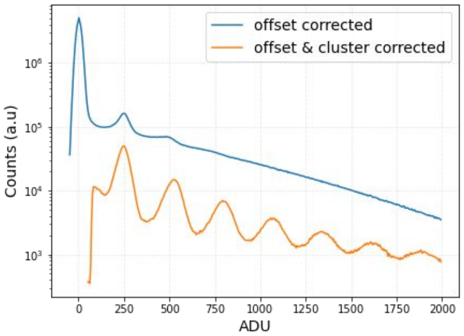

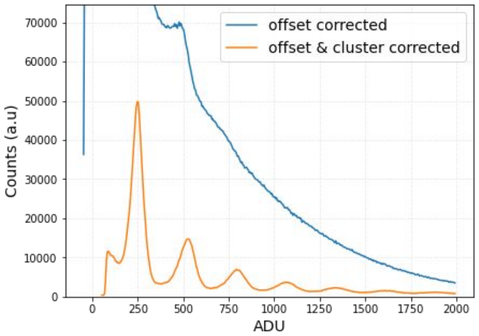

EPFL EUROfusion

Spectroscopic studies in the divertor of TCV's fusion plasmas

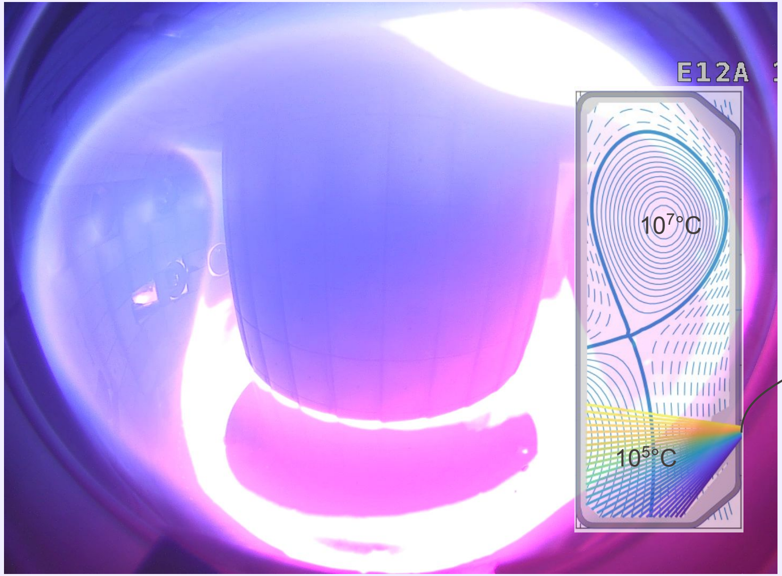

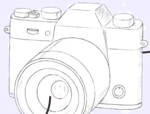

Raw data: visible light spectrum

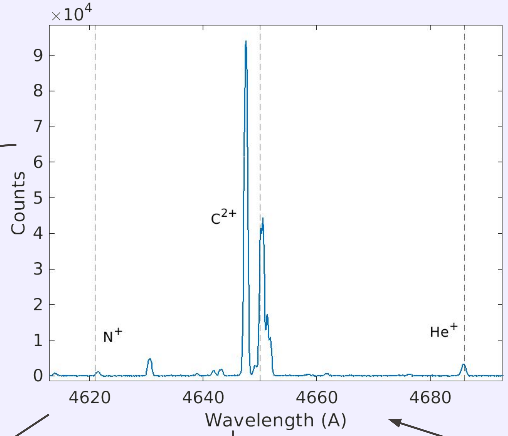

Modelling

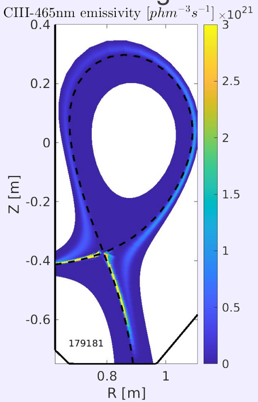

Spatial & temporal information

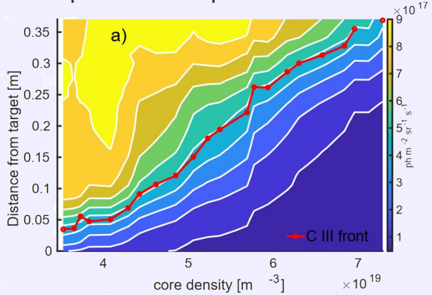

Ion temperature

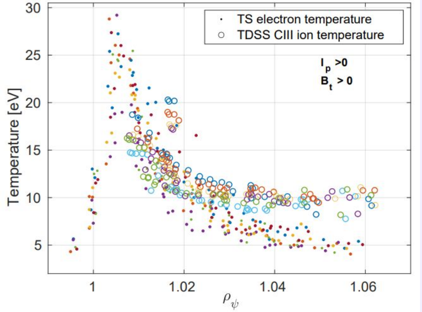

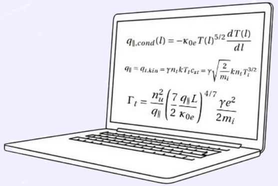

Richard Ducker

Karlsruhe Institute of Technology

Remote Handling Compatible In-bore Non-Destructive Examination for DEMO First Wall Cooling Pipes

Azman Azka M.Sc., Institute for Material Handling and Logistics

Motivation

- All pipe connection must pass inspection to be commissioned before operation is allowed to restart.
- Due to the difficult environmental condition, a remote handling compatible inspection method is developed to meet the challenges and requirement of operating inside DEMO reactor.
- Due to the design limitation of DEMO reactor, only in-bore inspection is feasible for the cooling pipe inspection.

Objective

- To Deploy relevant non-destructive testing sensor inside the pipe
- To find the relevant pipe joining location
- To monitor the internal condition of a pipe
- To assess the pipe defect
- To localise the location of critical defects on overall pipe layout

Method

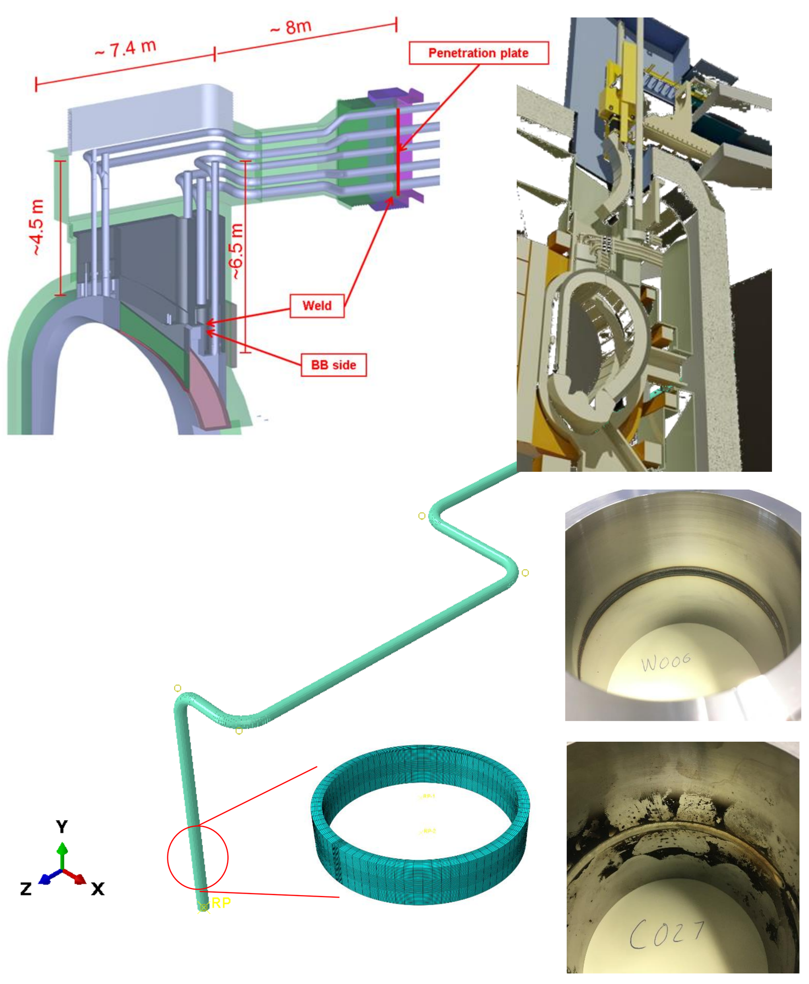

Weld location within overall upper port pipe forest

- A critical defect size (defect size which would lead to structural failure) is determined
- Study on the feasible inspection method for further development
- Development of deployment system for the relevant Inspection system.
- Preliminary testing of the inspection method on pipe sample
- Converting inspection result as data point
- Quantification of inspection result
- Localising defect data point on the digital twin of the reactor system

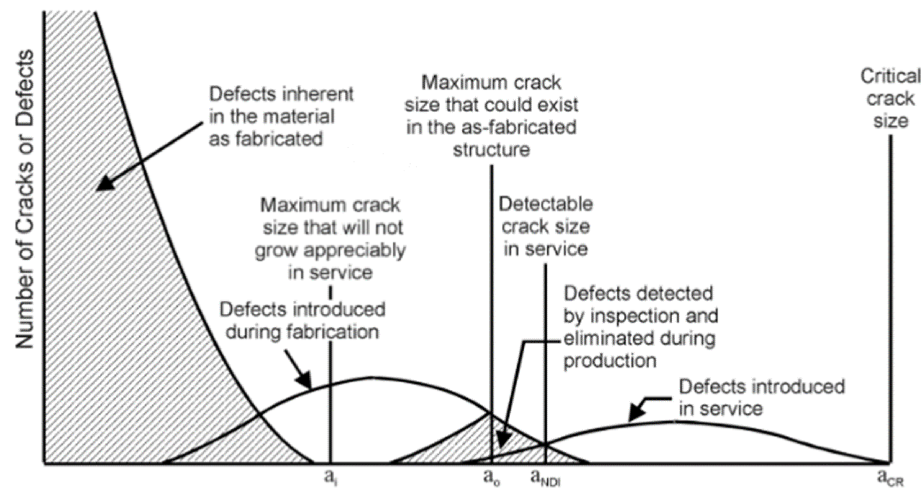

Critical defect size

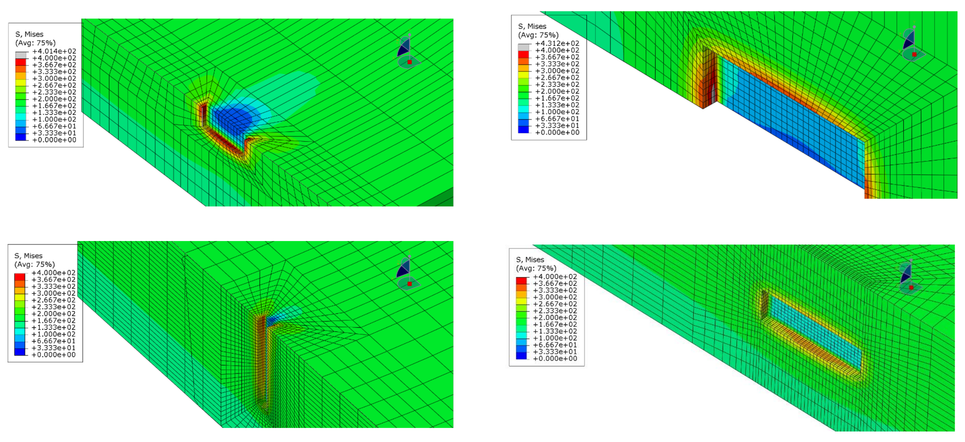

Numerical Study on critical defect size

Current Results

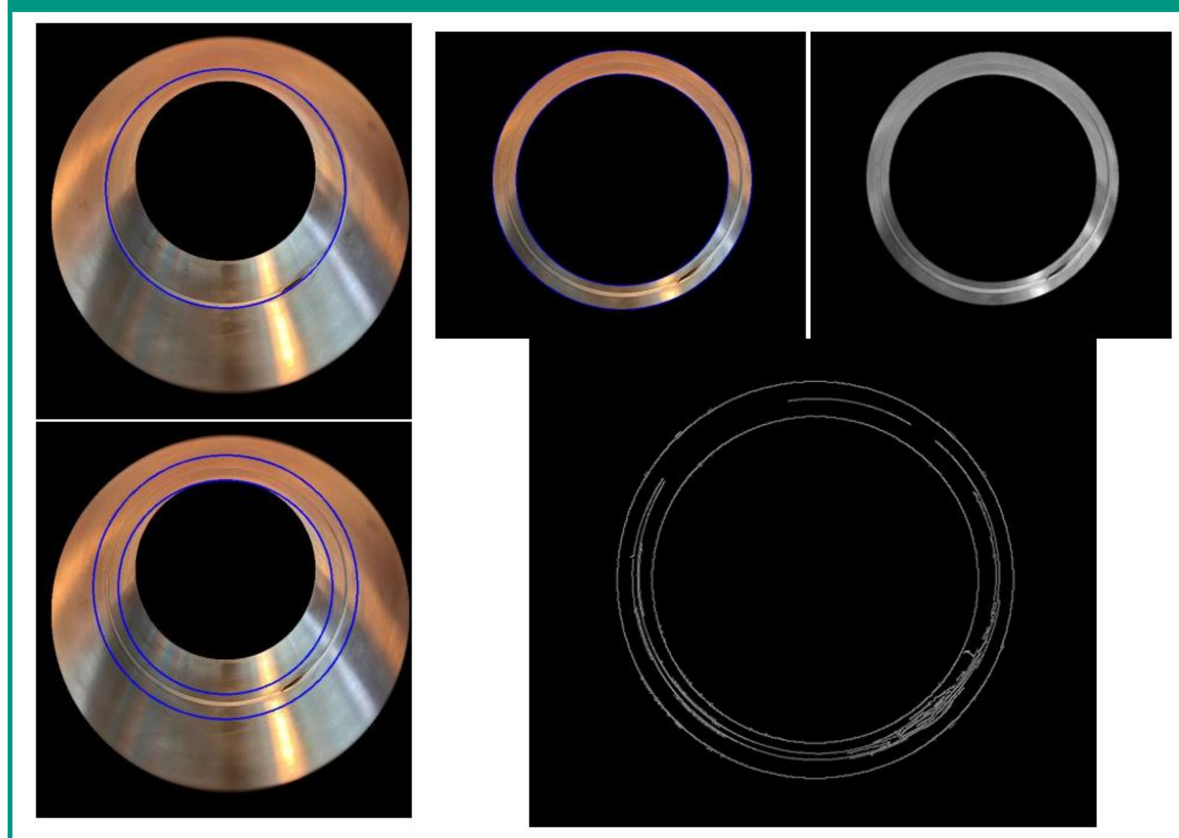

Detection of surface pipe defect using image processing

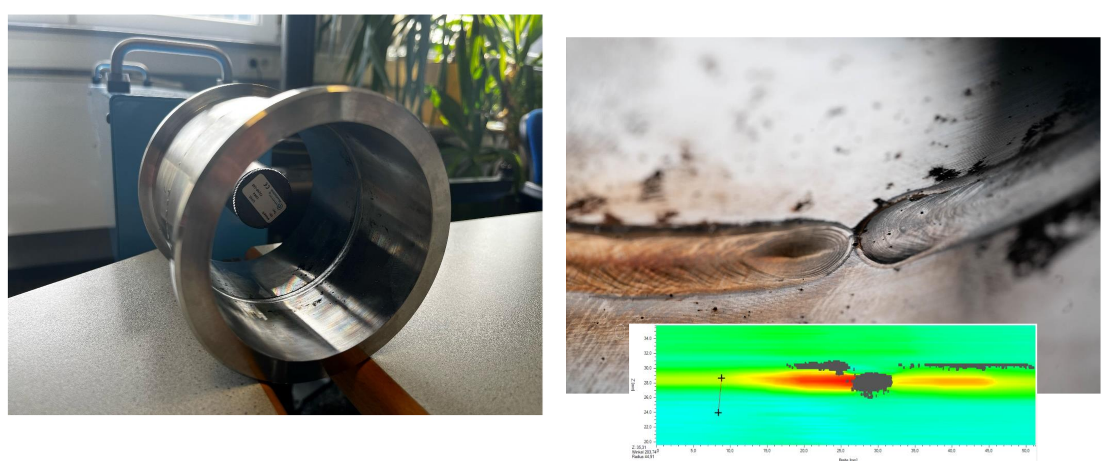

Detection of surface pipe defect using laser triangulation

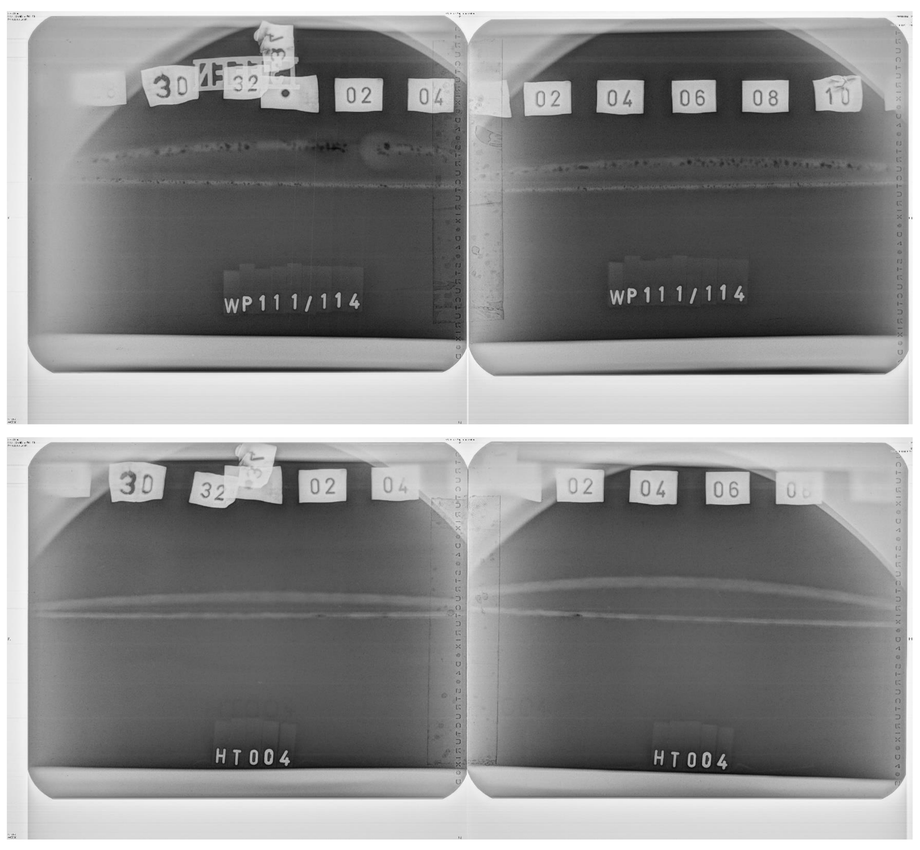

Volumetric testing using X-Ray as baseline

Outlook

- Application of SLAM to localise the defect location on the overall pipe layout
- Trial for visual inspection using synthetic samples to simulate various defects types which can occur in pipe welds
- Building a test rig to simulate pipe layout

Previous Test Rig at CCFE Culham for weld module deployment

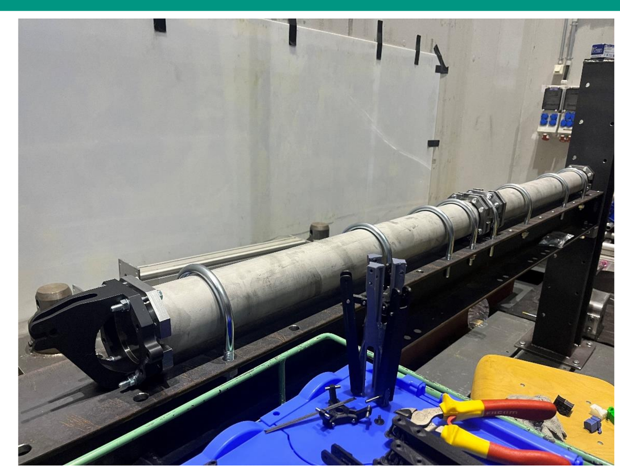

Current test Rig at KIT Karlsruhe for NDE unit model deployment (under construction)

EUROfusion

This work has been carried out within the framework of the EUROfusion Consortium, funded by the European Union via the Euratom Research and Training Programme (Grant Agreement No 101052200 — EUROfusion). Views and opinions expressed are however those of the author(s) only and do not necessarily reflect those of the European Union or the European Commission. Neither the European Union nor the European Commission can be held responsible for them.

8th EIROforum School on Instrumentation, 13-17 May 2024, Garching, Germany.

Development of Optical Emission Spectrometer (OES) for Impurity Monitoring in Thailand Tokamak 1 (TT-1)

Nopparit Somboonkittichai* (Kasetsart University, Thailand)

The TT-1 is equipped with only one visible CCD camera, where impurity radiation has been observed. The OES diagnostics is required for qualitatively and quantitatively monitoring impurity radiation. It is now designed and developed in Thailand by Thai researchers.

TT-1 and Preliminary OES: SPPT 2024, 17-20 June 2024, Prague, Czechia.

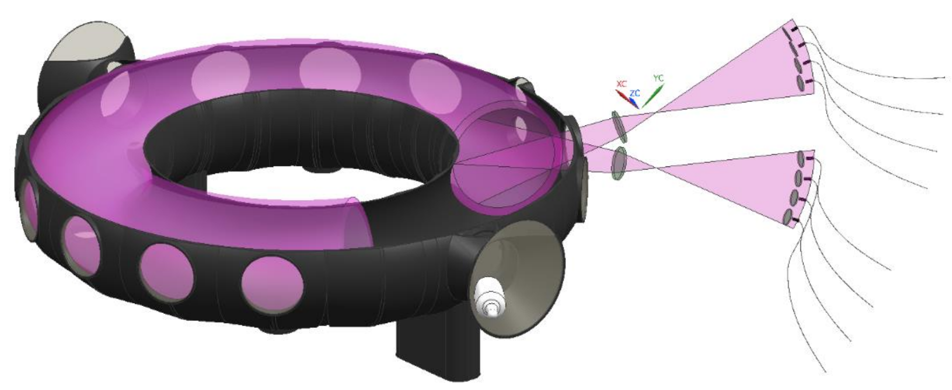

MHD Formulation for Partially Ionized Fusion Plasma

Nopparit Somboonkittichai* (Kasetsart University, Thailand)
Christopher Albert** (Fusion@ÖAW, ITPCP, TU Graz, Austria)

Partially ionized plasma can be found in:

1. edge fusion plasma, and
2. low temperature plasma.

Full kinetic equations need more power for computation. This inspires to adopt an MHD scheme with an acceptable accuracy.

Equations of Motion:

(N. Somboonkittichai, C. Albert *et al* in preparation 2024)

1. Rate equations of ions and neutrals with excitations and ionizations by electrons,

2.Momentum equations of MHD and neutral fluids with "**j×B**" force & a drag force due to ion-neutral collisions,

3.Energy equations of ions, electrons and neutrals.

Emails: nopparit.so@ku.th*, fscinrso@ku.ac.th*, albert@tugraz.at**
(See the full list of collaborators of both works in the poster)

MICADO Cryogenic Control Software

Sriprasanna Annadevara, Hanna Kellermann

University Observatory Munich, Scheinerstr. 1, 81579 Munich, Germany

What is our poster about?

- PLC-based control software
- Managing about 180 cryostat devices

What cryostat?

- Cryostat housing MICADO
- 4890 l cryostat kept at 10^{-6} mbar and 82°K

What is MICADO?

- MICADO - Multi-AO Imaging Camera for Deep Observations
- First-light instrument for ESO’s ELT (Extremely Large Telescope)
- NIR imager and spectrograph

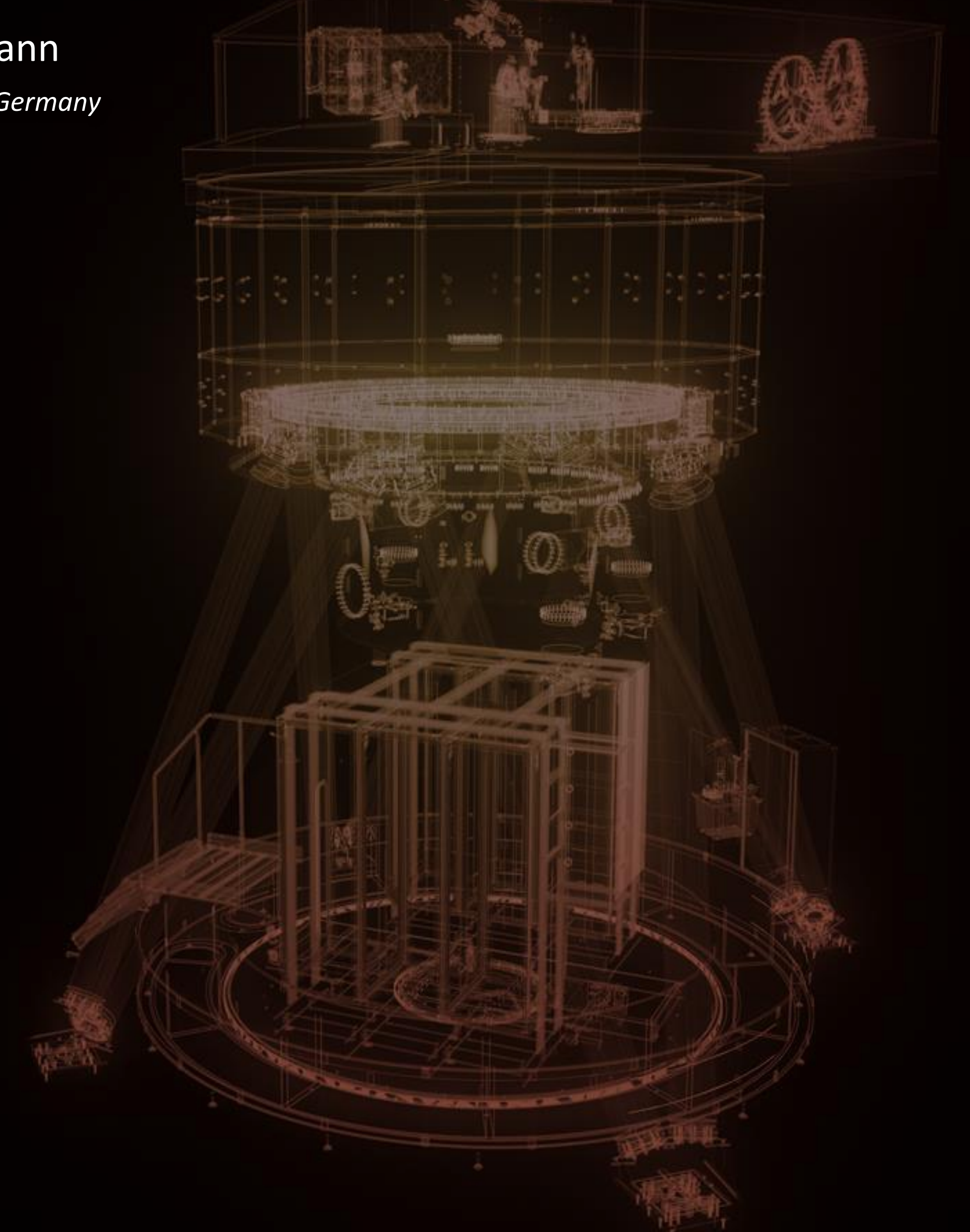

The timing arrangement of the XFEL beam is crucial in determining the specifications needed for X-ray detectors

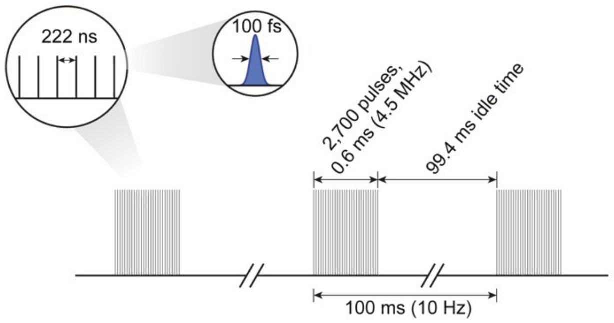

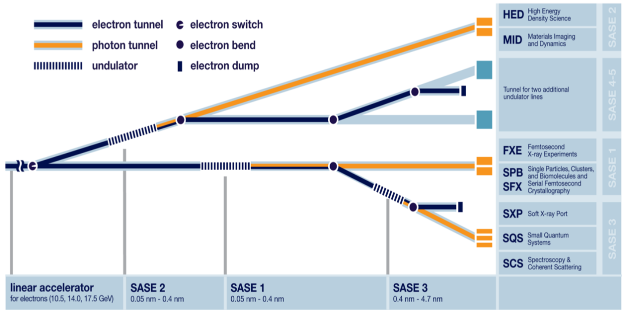

* XFEL.eu Webpage. Accessed: Apr. 3, 2024. [Online]. Available: https://www.xfel.eu/facility/overview/index_eng.html

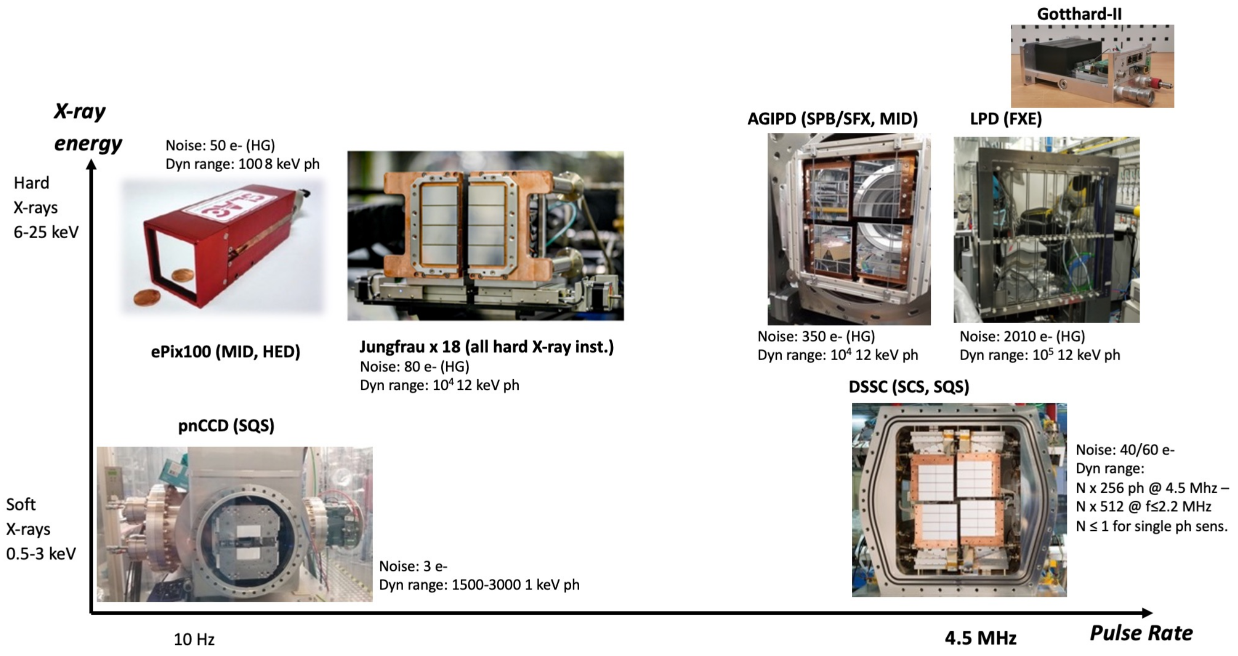

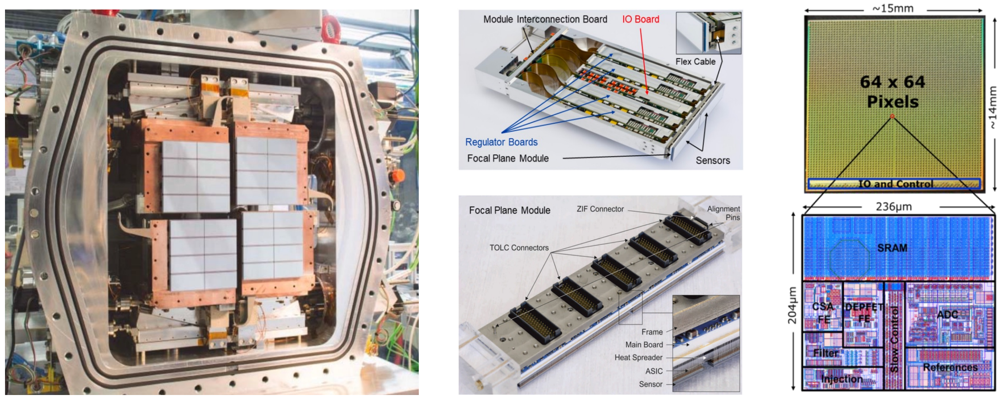

* Porro, Matteo, et al. "The MiniSDD-based 1-Mpixel camera of the DSSC project for the European XFEL." *IEEE Transactions on Nuclear Science* 68.6 (2021): 1334-1350.

Detector Development at European XFEL

- Enhance internal XFEL proficiency in critical detector development assignments. Get more involved in detector electronics development, ASIC design and the FPGA firmware development.
- Replace the discontinued and EOL components to insure safe operation in future.
- Final goal: develop new generation detectors: optimization of existing detector systems, developments based on the existing main hardware components (smaller pixel, wider energy range).

EIROforum School on Instrumentation 2024

Unravelling Gain Characterisation of the AGIPD

Vratko Rovensky, Jolanta Sztuk-Dambietz, Karim Ahmed, Olivier Meyer, Andrea Parenti, Natascha Raab, Marcin Sikorski, Monica Turcato

Introduction

The European X-ray Free Electron Laser (EuXFEL)

- Scientific User facility, in operation since 2017
- Three SASE beamlines, seven experimental stations serving energies from 260 eV to 25 keV
- High brilliance, ultra-short spatially coherent X-ray pulses delivered up to 4.5 MHz repetition rate
- Requirements for detector: compatible with XFEL time structure, high dynamic range, single photon sensitivity, radiation hard
- Three dedicated detector projects for the EuXFEL: **AGIPD**, DSSC, LPD

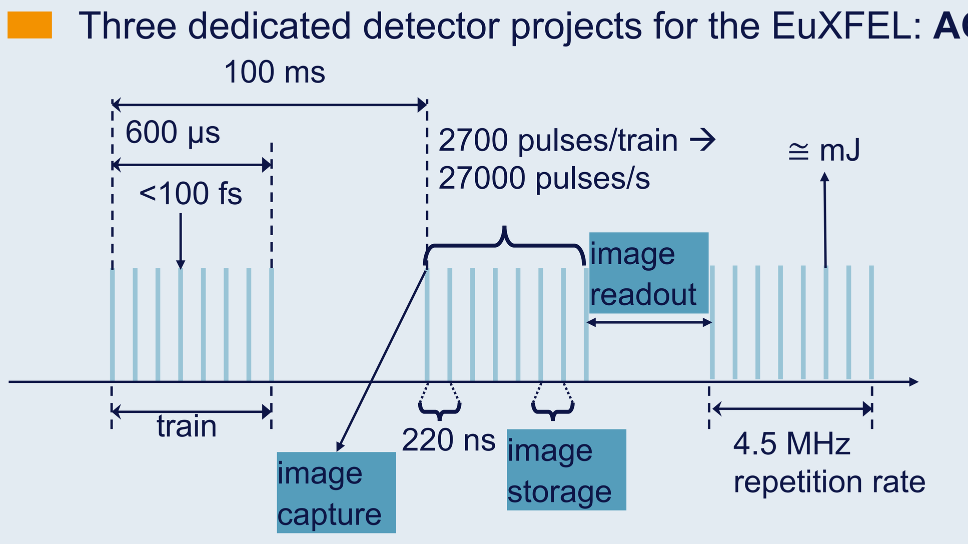

Fig. 1: EuXFEL pulse delivery characteristics.


Fig. 2: AGIPD1M at SPB/SFX instrument.

The Adaptive Gain Integrating Pixel Detector – AGIPD

- 1 Mpixel hybrid camera
- 4.5 MHz integration with on-pixel storage (352 memory cells) during burst period
- Single photon sensitivity & dynamic range of >10^3 ph/pixel at 12 keV → three adaptive gain stages
- Used at SPB/SFX, MID, HED (AGIPD500K)

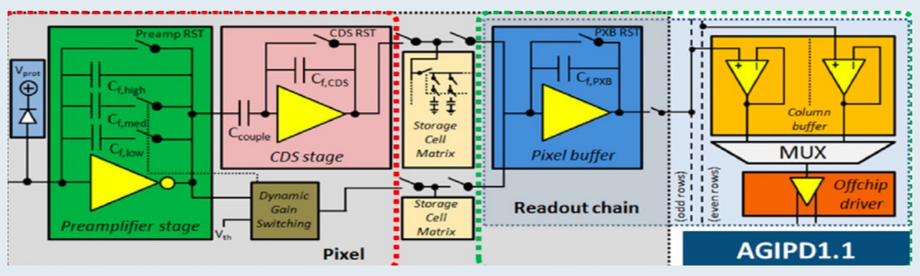

Fig. 3: Schematic of the AGIPD pixel. Adopted from [2].

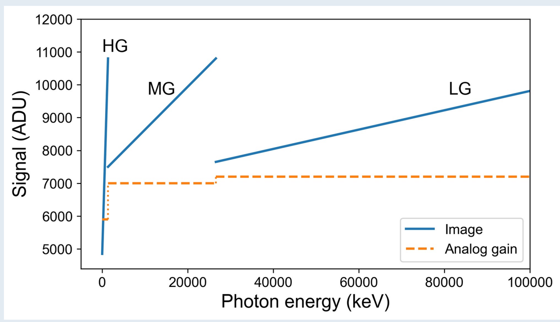

Fig. 4: AGIPD1M dynamic range visualization.

Gain Calibration

Strategy

- High Gain (HG) – absolute calibration with low intensity X-ray fluorescence flat-fields → **Absolute gain correction**
- Medium Gain (MG), Low Gain (LG) – relation of gain stages to HG determined by dynamic range scans with internal charge injection sources → **Relative gain correction**
- Absolute calibration of the entire dynamic range with X-rays not feasible

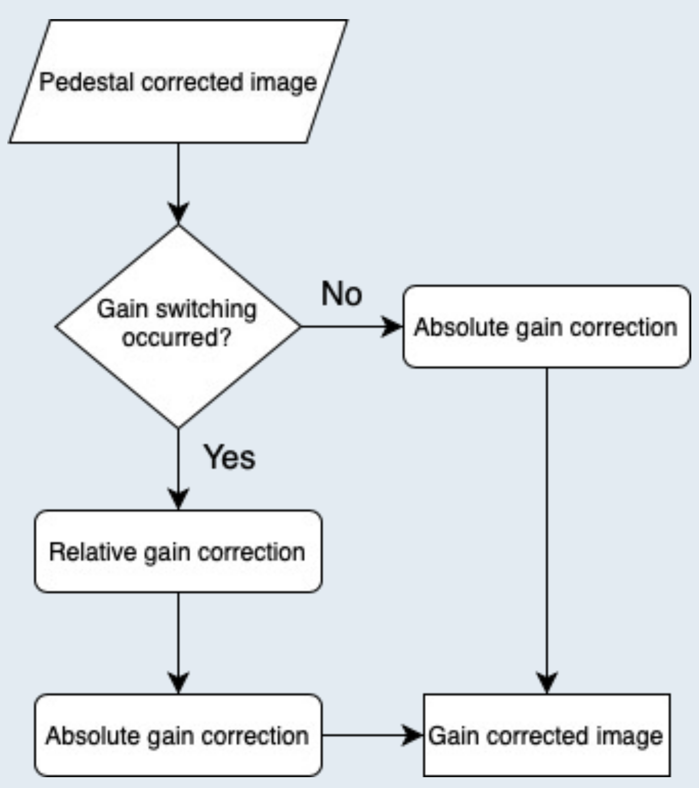

Fig. 5: Simplified flowchart of gain correction steps.

High Gain Calibration

- Performed bi-annually with a defocused XFEL beam
- Typically X-ray fluorescence of Cu target
- Low intensity flat-fields - ca. 0.5 ph/pixel/pulse
- Measured fluorescence spectrum modeled with multi-Gaussian function (Fig. 6)
- Absolute gain constant - separation between photon peak positions determined for each pixel and memory cell (Fig. 7)

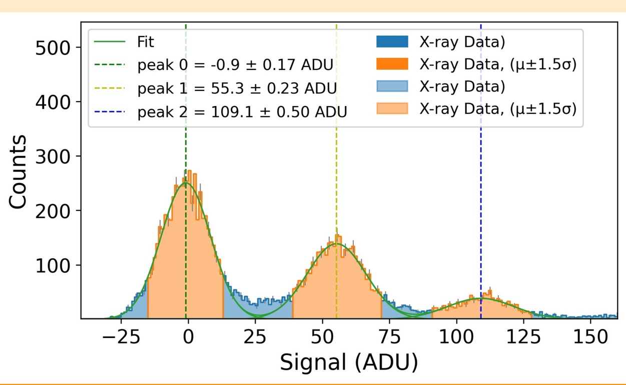

Fig. 6: Cu fluorescence measured for a single pixel and memory cell.

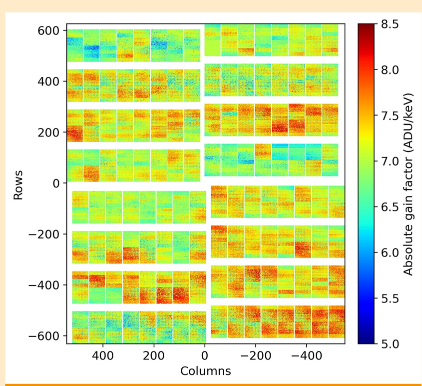
Fig. 7: Example of absolute gain map.

Medium & Low Gain Calibration

- Two internal calibration sources: pulsed capacitor PC (used routinely), current source CS (newly integrated in the EuXFEL infrastructure)
- Measured signal fitted with linear function for each gain stage separately (Fig. 8, 9)
- Relative gain constant – ratio of gain stages slopes for each memory cell in every pixel
- Average values of gain slope ratios:
  - PC: HG/MG = 33.5 ± 1.9
  - CS: HG/MG = 37.5 ± 3.6, MG/LG = 4.3 ± 0.5

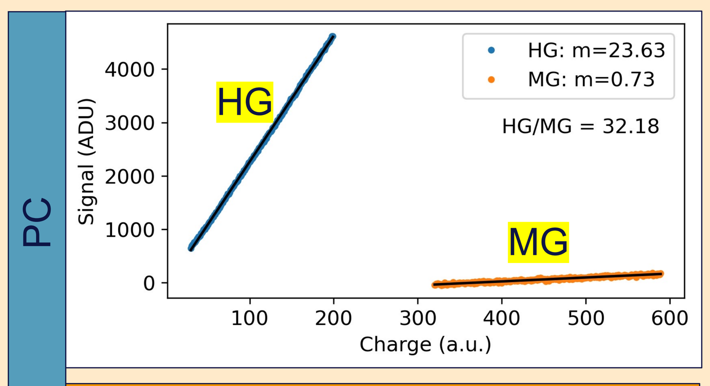

Fig. 8: Linear fits to PC signal.

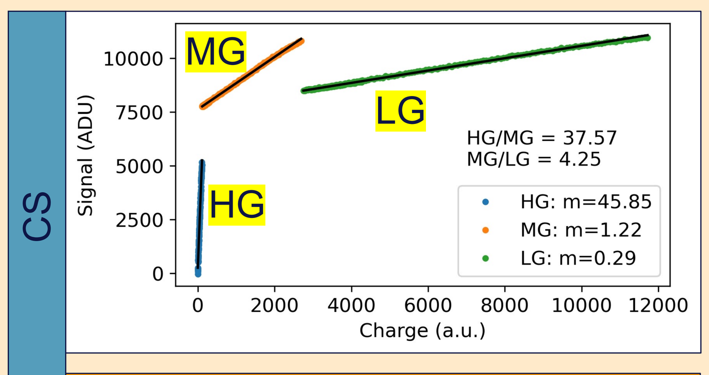

Fig. 9: Linear fits to CS signal.

Pulsed Capacitor vs. Current Source

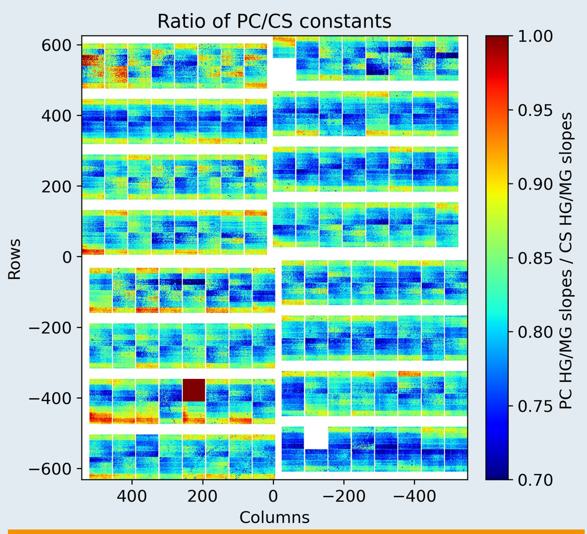

Fig. 10: Ratio of PC and CS constants for cell 1.

Memory cell dependencies

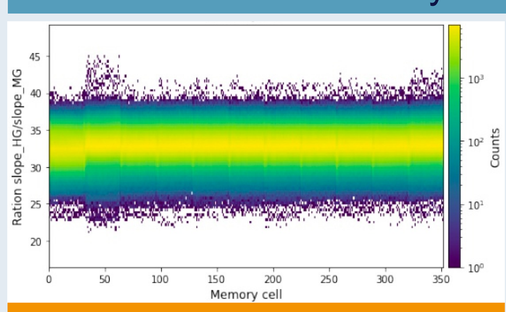
Fig. 11 PC - HG slope / MG slope

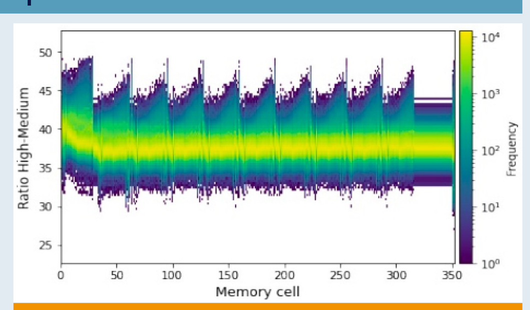
Fig. 12: CS - HG slope / MG slope

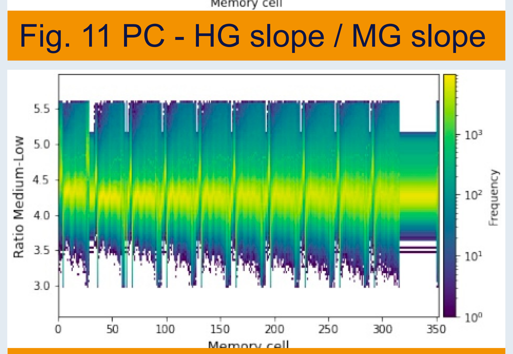
Fig. 13: CS - MG slope / LG slope

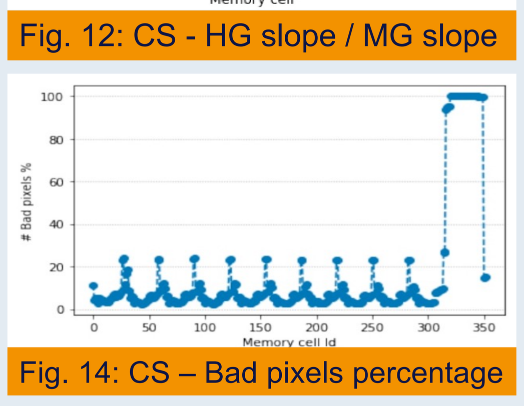
Fig. 14: CS – Bad pixels percentage

Gain Correction of Image

Water diffraction

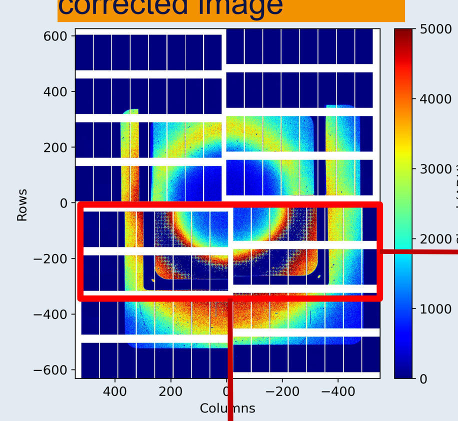
Fig. 15: Pedestal corrected image

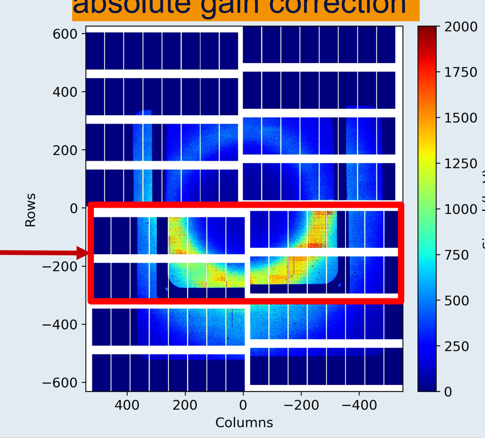
Fig. 17: Relative (PC) & absolute gain correction

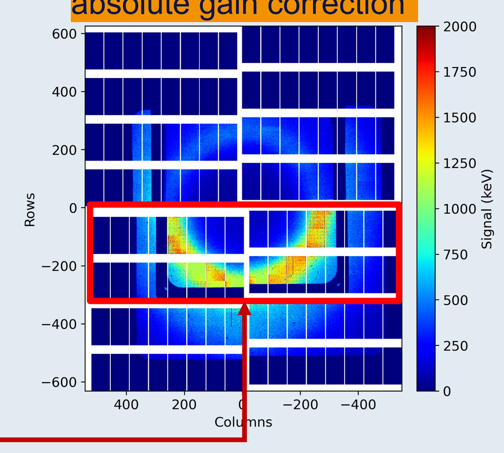
Fig. 18: Relative (CS) & absolute gain correction

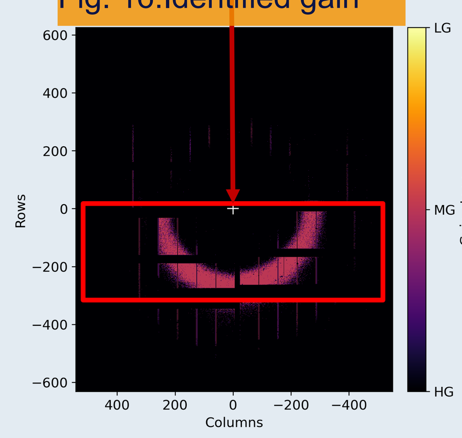
Fig. 16:Identified gain

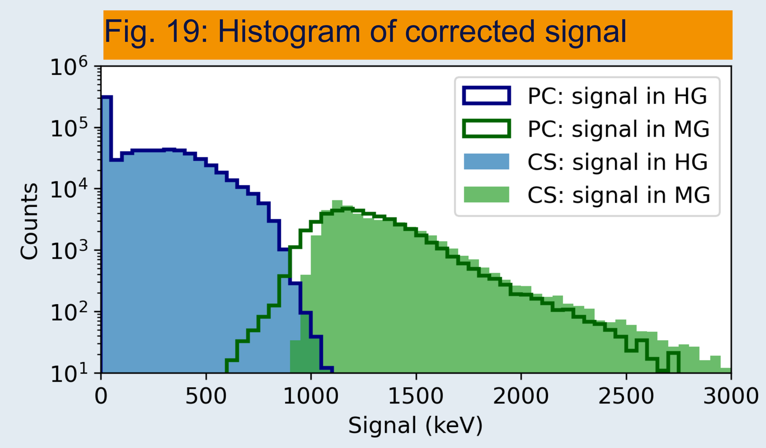

Fig. 19: Histogram of corrected signal

Summary

- Both charge injection sources are now available for the AGIPD gain corrections
- PC limitations: scans only through HG and part of MG
- Validation and characterization of the current source for calibration is a work in progress
  - More datasets required to fully characterise AGIPD1M with CS scan
  - Current source relative gain constants are on average higher by ~12%

References

1. Sztuk-Dambietz, Jolanta, et al. "Operational experience with adaptive gain integrating pixel detectors at European XFEL." Frontiers in Physics 11 (2024): 1329378
2. Mezza, D., et al. "Calibration methods for charge integrating detectors." Nuclear Instruments and Methods in Physics Research Section A: Accelerators, Spectrometers, Detectors and Associated Equipment 1024 (2022): 166078.

European XFEL GmbH, Vratko Rovensky, Holzkoppel 4, 22869 Schenefeld, Germany, Phone +49 40 8998-6805, Fax +49 40 8998-1905, vratko.rovensky@xfel.eu
www.xfel.eu

ENLIGHTENING SCIENCE